Sedimentology and chronostratigraphy of the Apt Basin, Southeastern France: lacustrine response to late Paleogene cooling and regional rifting

Alexis Licht, Pauline Coster, Paul Botté, Mustafa Kaya, Pierre Deschamps, Abel Guihou, Stéphane Legal

BSGF - Earth Sciences Bulletin 2024, 195, 22
© A. Licht *et al.*, Published by EDP Sciences 2024
https://doi.org/10.1051/bsgf/2024019

BSGF Earth Sciences Bulletin
Available online at:
www.bsgf.fr

OPEN ACCESS

Sedimentology and chronostratigraphy of the Apt Basin, Southeastern France: lacustrine response to late Paleogene cooling and regional rifting

Alexis Licht[1,*], Pauline Coster[2], Paul Botté[1], Mustafa Kaya[3], Pierre Deschamps[1], Abel Guihou[1] and Stéphane Legal[2]

[1] Aix-Marseille Univ., CNRS, IRD, INRAE, CEREGE, Aix-en-Provence, France
[2] Réserve Naturelle Nationale Géologique du Luberon, Parc naturel régional du Luberon, 60 Place Jean Jaurès, 84400 Apt, France
[3] Middle East Technical University, Department of Geological Engineering, Ankara, Turkey

Received: 15 April 2024 / Accepted: 28 August 2024 / Publishing online: 1 November 2024

Abstract – The Apt Basin, sub-basin of the wider Manosque Basin of southeastern France, contains deposits of Eocene-Oligocene lake systems that were part of a broader network of evaporative lakes and lagoons spread across the European Cenozoic rift system. The onset and mechanisms of subsidence in the rift system, the interconnectivity of these lakes, and their response to the transition into the Oligocene icehouse are poorly understood. This study aims to clarify these points by examining the stratigraphy and depositional environments in the Apt Basin. We correlate and date Eocene to lowermost Oligocene geological units using a basin-wide facies model combined with sedimentological and geochronological approaches. We show the existence of three lacustrine phases, each separated by complete lake drying events: (1) an Ypresian (?) – Lutetian lake-marsh system dominated by palustrine carbonates; (2) a Bartonian (?) – Priabonian siliciclastic fluvio-deltaic and saline lake system; and (3) a lower Rupelian saline carbonate lake system. The presence of a lake system during the Ypresian (?) – Lutetian suggests an onset of basin subsidence before most other basins of the rift system in southeastern France, and is associated with the late Pyrenean deformation phase. The initiation of the second lacustrine phase marks the beginning of E-W extension and the formation of the Apt Basin as an individual horst & graben system. Based on facies distribution, we demonstrate the hydrological isolation of the Apt Basin from other basins and the improbability of any marine connection during the first two phases. This isolation is less certain for the third phase. We show a close synchronicity between the second lake drying event and the Eocene-Oligocene Transition. The third lacustrine phase, dominated by carbonate production and low siliciclastic input, is interpreted as reflecting a long-term decrease in surface runoff associated with the fall into the Oligocene icehouse.

Keywords: Eocene-Oligocene Transition / Carbonate U-Pb dating / continental sedimentology / Basin geology

Résumé – Sédimentologie et chronostratigraphie du bassin d'Apt, Sud-Est de la France : réponse des systèmes lacustres provençaux aux refroidissements tardi-paléogènes et au rifting régional Le Bassin d'Apt, sous-bassin du Bassin de Manosque dans le Sud-Est de la France, contient des dépôts lacustres d'âge éocène et oligocène qui font partie d'un plus large réseau de lacs évaporatifs et de lagons anciens répartis le long du système de rift cénozoïque ouest-européen. Le démarrage et les mécanismes de subsidence de ces bassins, l'interconnectivité de ces lacs et leur réponse à la chute climatique dans l'Oligocène glaciaire sont encore peu compris. Cette étude a pour but de documenter ces points en clarifiant la stratigraphie et les environnements de dépôt du Bassin d'Apt. Nous corrélons et datons les formations géologiques d'âge éocène et oligocène inférieur en utilisant un modèle de faciès à l'échelle du bassin et une combinaison d'approches sédimentologiques et géochronologiques. Nous montrons l'existence de trois phases lacustres séparées par des épisodes d'assèchement complet du lac : (1) un système lacustre marécageux d'âge Yprésien (?) – Lutétien dominé par les carbonates palustres ; (2) un système fluvio-deltaïco-lacustre salin à fort apport siliciclastique d'âge Bartonien (?) – Priabonien ; et (3) et un système

*Corresponding author: licht@cerege.fr

lacustre salin dominé par la sédimentation carbonatée, d'âge Rupélien inférieur. L'existence d'un premier système lacustre durant l'Yprésien (?) – Lutétien indique un démarrage de la subsidence du Bassin d'Apt bien avant la plupart des autres bassins du rift ouest-européen et est associée à un épisode local de déformation tardi-pyrénéen. L'initiation de la deuxième phase lacustre marque le démarrage de l'extension régional Est-Ouest et la formation du Bassin d'Apt comme partie intégrante d'un système de horst & graben. La distribution des faciès fluvio-deltaïques montre un isolement hydrologique complet du lac et suggère l'absence de toute connexion avec la mer durant les deux premières phases lacustres. Cet isolement est moins clair pour la troisième phase. Nous montrons une proche synchronicité entre l'assèchement final de la deuxième phase lacustre et la transition Eocène-Oligocène. La troisième phase lacustre, dominée par la production carbonatée et à faible apport siliciclastique, est interprétée comme reflétant une baisse durable du ruissellement de surface associée à la chute dans l'Oligocène glaciaire.

Mots clés : Transition Eocène-Oligocène / Datation U-Pb des carbonates / sédimentologie continentale / Géologie de bassin

1 Introduction

The Manosque Basin of southeastern France (also known as the Apt-Forcalquier Basin) is part of the European Cenozoic Rift System (ECRIS; Dèzes *et al.*, 2004). It hosts Eocene-Oligocene fluvio-lacustrine deposits capped by lower to middle Miocene shallow marine marls and bioclastic sands (Gigot *et al.*, 1975; Lesueur *et al.*, 1990). The Paleogene lake systems of the Manosque Basin were part of a much wider network of evaporative lakes and lagoons spread over ECRIS basins in southeastern France and the Rhone Valley Fig. 1 (Triat and Truc, 1974; Sissingh, 2001; Nury *et al.*, 2016; Lettéron *et al.*, 2017; Semmani *et al.*, 2022). The onset and mechanisms of ECRIS basin subsidence in southeastern France, the inter-connectivity of these lakes, a possible connection to the sea, the origin of their evaporative deposits, and the influence of late Eocene-early Oligocene global cooling on their evolution are poorly understood and have been the focus of several recent studies in neighboring basins (Alès Basin: Letteron *et al.*, 2022; Vistrenque Basin: Semmani *et al.*, 2023). The Manosque Basin remains yet poorly studied in the light of these questions, and no stratigraphic nor sedimentological work on its Paleogene deposits has been carried out since the PhD thesis of Lesueur (1991).

The Manosque Basin developed as a graben system following a regional E-W extension phase starting in the late Eocene (Gigot *et al.*, 1977). It is divided into two sub-basins: the Forcalquier Basin to the east and the Apt Basin to the west, separated by a horst running along Flaqueirol Pass (Fig. 2). Both sub-basins were occupied by individual lake systems for the Eocene – earliest Oligocene, until their unification into a single lake system during the middle Rupelian (Lesueur, 1991). The Apt Basin is famous for yielding several prolific fossil sites including the Débruge locality (latest Eocene, type locality for mammalian biohorizon MP18; de Bonis, 1963), the Murs locality (MP23) first studied by Stehlin (Rémy, 2000; Costeur *et al.*, 2019), early Oligocene insect, plant and fish-yielding sites (Coster and Legal, 2021; Nel *et al.*, 2023), and the iconic fossil footprint site of Saignon (Belvedere *et al.*, 2023; see review of sites in Ménouret, 2014). The first detailed descriptions of the different lithostratigraphic units of the Apt Basin were published in the 1960s and 1970s (Truc and Demarcq, 1967; Roch 1971; Triat and Truc, 1974). Geological mapping of the Apt Basin split the area into three 1:50,000 maps that unfortunately use different names and lithostratigraphic definitions for the Eocene-Oligocene geological units (Goguel *et al.*, 1966; Germain *et al.*, 1966; Blanc *et al.*, 1975). This paper aims at clarifying the stratigraphy of the Apt Basin for the geological units preceding the integration of its lacustrine system with the one of the Forcalquier Basin during the middle Rupelian. We correlate and date Eocene-lowermost Oligocene geological units of the Apt Basin in order to better understand the chronology and connectivity of the regional lake systems.

2 Geological context

2.1 The wider Manosque Basin

The Eocene to Miocene Manosque Basin developed as a graben system on the wider Mesozoic Provence Basin, following a 50 Myr-long regional hiatus of sedimentation associated with the Durance uplift episode and Pyrenean deformation (Bestani *et al.*, 2016). It is bound to the north by the Vaucluse Range and the Lure Mountain, and to the south by the Luberon Range, where limestones of the Cretaceous Urgonian carbonate platform of southeastern France make most of the exposed rocks (Léonide *et al.*, 2012). The Luberon Range is an E-trending, south-verging ramp anticline mainly developed during the Eocene Pyrenean phase of deformation; a later shortening phase during the Miocene resulted in further uplift and folding of the range and the folding of the central part of the Manosque Basin into an associated E-trending syncline (Clauzon *et al.*, 2011). The Manosque Basin is bound to the east by the Middle Durance Fault Zone and to the west by the Cavaillon Fault Zone (Fig. 2). The Middle Durance Fault Zone is a long-lived NNE-trending fault network which marks the eastern border of the Mesozoic Provence Basin (Baudrimont and Dubois, 1977); in the latest Eocene – Oligocene, it was acting as a normal fault and formed the eastern margin of the Forcalquier Basin (Gigot *et al.*,1977; Guyanot-Benaize *et al.*, 2015). The Cavaillon Fault is also a long-lived NNE-trending fault that today marks the eastern boundary of the Cenozoic Carpentras Basin in the Rhone Valley (Molliex *et al.*, 2011). During Eocene-Oligocene times, the area directly to the east of Cavaillon Fault has been proposed to form a local horst and a paleo-high separating the Apt Basin from the Carpentras Basin, based on facies

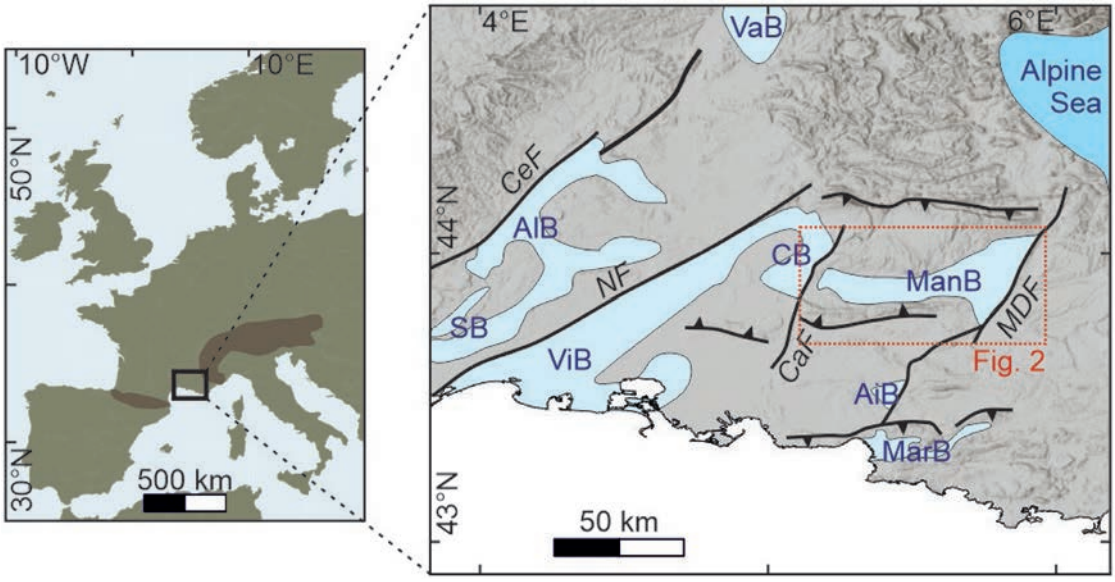

Fig. 1. Location of the study area and extent of the onshore basins and main fault systems of southeastern France during the late Eocene – early Oligocene, after Semmani *et al.* (2023). In blue, extent of upper Eocene – lower Oligocene sedimentary deposits of ECRIS basins and the Alpine Sea: VaB (Valence Basin), AlB (Alès Basin), SB (Sommières Basin), ViB (Vistrenque Basin), CB (Carpentras Basin), ManB (Manosque Basin), AiB (Aix Basin) and MarB (Marseille Basin). Main fault systems are displayed by black lines: CeF (Cévennes Fault), NF (Nimes Fault), CaF (Cavaillon Fault), MDF (Middle Durance Fault). The location of Fig. 2 is displayed by a red dotted square; the Apt Basin is a sub-basin of the Manosque Basin.

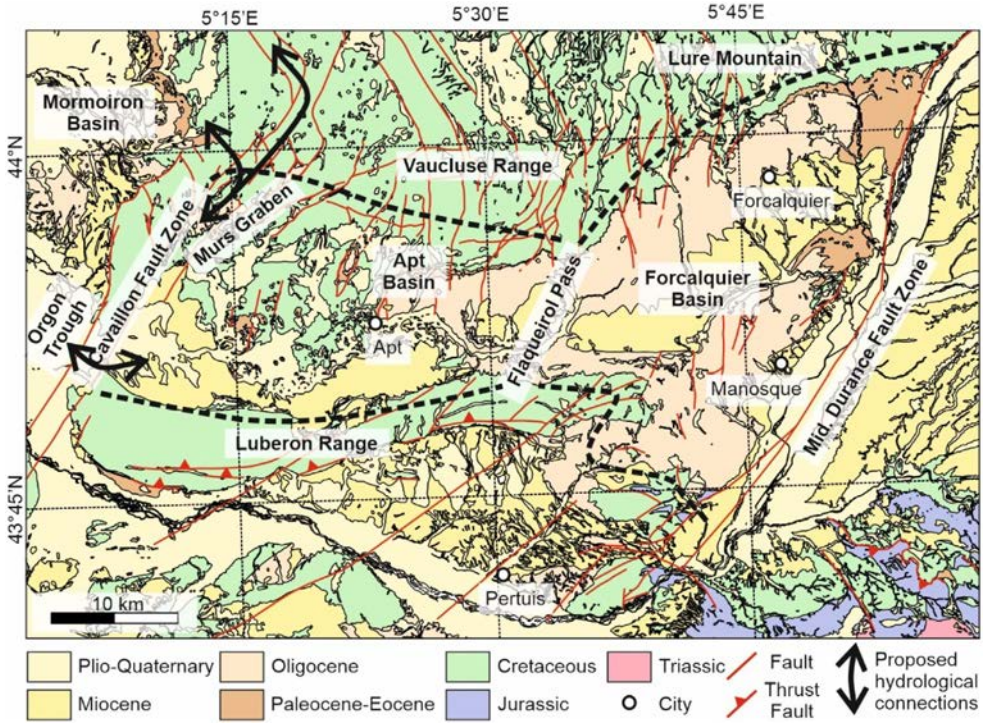

Fig. 2. Regional geological map of the Manosque Basin and its two sub-basins (Apt and Forcalquier Basins), highlighting the localities and geological features discussed in the text (modified after SIT-PNR-PACA-Luberon, http://sit.pnrpaca.org/pnr_geologie/index.html).The extent of the Apt and Forcalquier sub-basins, separated by Flaqueirol Pass, is shown with thick dashed lines. Black arrows show the proposed hydrological connections between the Apt Basin and the ECRIS basins further west.

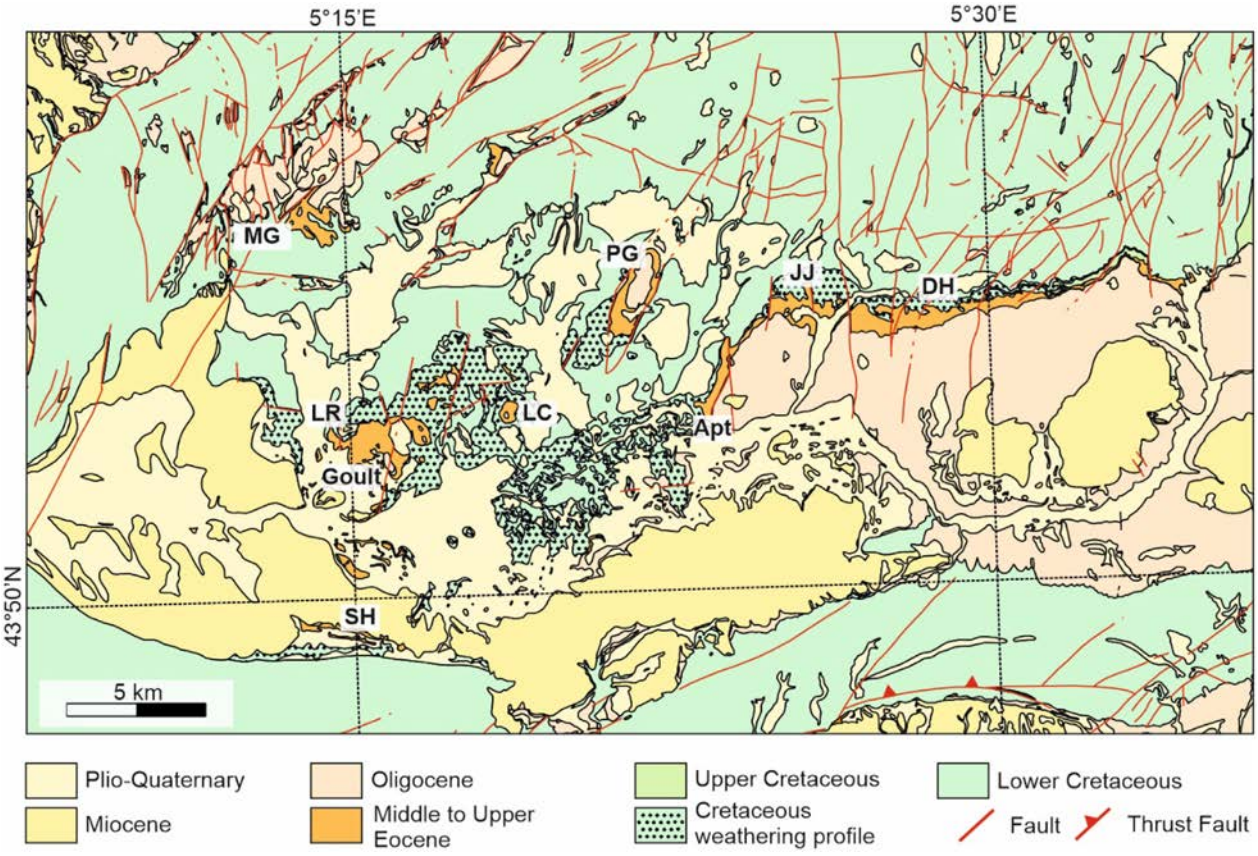

Fig. 3. Geological map of the Apt Basin (modified after SIT-PNR-PACA-Luberon, http://sit.pnrpaca.org/pnr_geologie/index.html), highlighting the name of the nine localities discussed in the text: Murs village (in the Murs Graben; MG), La Rabotte farm (LR), Goult village, Saint Hilaire monastery (SH), La Coquillade hill (LC), the Perréal Graben (PG), Apt city, Jean-Jean hamlet in Apt (JJ), and the Dog Head cliff (DH).

distribution (Triat and Truc, 1974). Two potential hydrological connections have been proposed between the lakes of the Manosque Basin and the western sub-basins of the Carpentras Basin (the Orgon Trough and the Mormoiron Basin; Truc, 1978): (1) to the west of the Apt Basin across the Cavaillon Fault zone, towards the Orgon Trough; (2) and to the northwest of the Apt Basin via the northern end of the Murs Graben, towards the Mormoiron Basin (Fig. 2).

The uppermost part of the Mesozoic basement in the Manosque Basin forms a classical sequence that is found regionally: Barremian-Aptian Urgonian limestones are overlain by Aptian marls, overlain by Albian-lower Cenomanian marls and glauconitic sands. These glauconitic sands are the ultimate deposits of a regional regressive sequence associated with the Durance uplift episode that exposed most of the Mesozoic Provence Basin during the early Cenomanian (Conard-Noireau, 1983). West of Flaqueirol Pass, in the northern part of the Apt Basin, thin (<20 m) lenses of continental sandstones of hypothetical Turonian age cap the Albian-Cenomanian glauconitic sands (*Pied Bousquet Sandstones*; in French: *Grès de Pied Bousquet*; Clauzade *et al.*, 1962); a thick (>30 m), polygenetic weathering profile has then developed on top of the sequence, yielding to the ochrification of the glauconitic sands, the formation of iron crusts and ulterior silcretes at the top of the profile (Triat, 1983). The southern part of the Apt Basin lacks Albo-Cenomanian deposits and the weathering profile is expressed as a thick karstic surface developed in the Urgonian limestones ("Coulon Paleokarst"; Guendon, 1981, Triat, 1982). East of Flaqueirol Pass in the Forcalquier Basin, the weathering profile is absent and marine deposits persist until at least the middle Cenomanian (Goguel *et al.*, 1966). These changes indicate that Flaqueirol Pass has been a persisting paleogeographic boundary since at least the Cretaceous (Triat, 1983); it is possibly representing an ancient N-trending fault network mirroring the Cavaillon and Middle Durance Fault Zones, northern bound of which can be tracked in the foothills of Lure Mountains ("Champs de Banon"; Joseph *et al.*, 1987), and that is nowadays inactive.

2.2 Stratigraphy of the Apt Basin

The Apt Basin groups all Cenozoic deposits west of Flaqueirol Pass and east of the Cavaillon Fault Zone. It includes two local smaller grabens (Fig. 3): (1) the Perréal Graben, today exposed by inverted topography, stratigraphy of which has been particularly studied because it has yielded the famous Débruge fauna (de Bonis, 1963; Truc and Demarcq, 1967); (2) the Murs Graben, at the northwest edge of the basin. When the base of the Cenozoic section is observable, Cenozoic deposits unconformably overlay the Cretaceous weathering

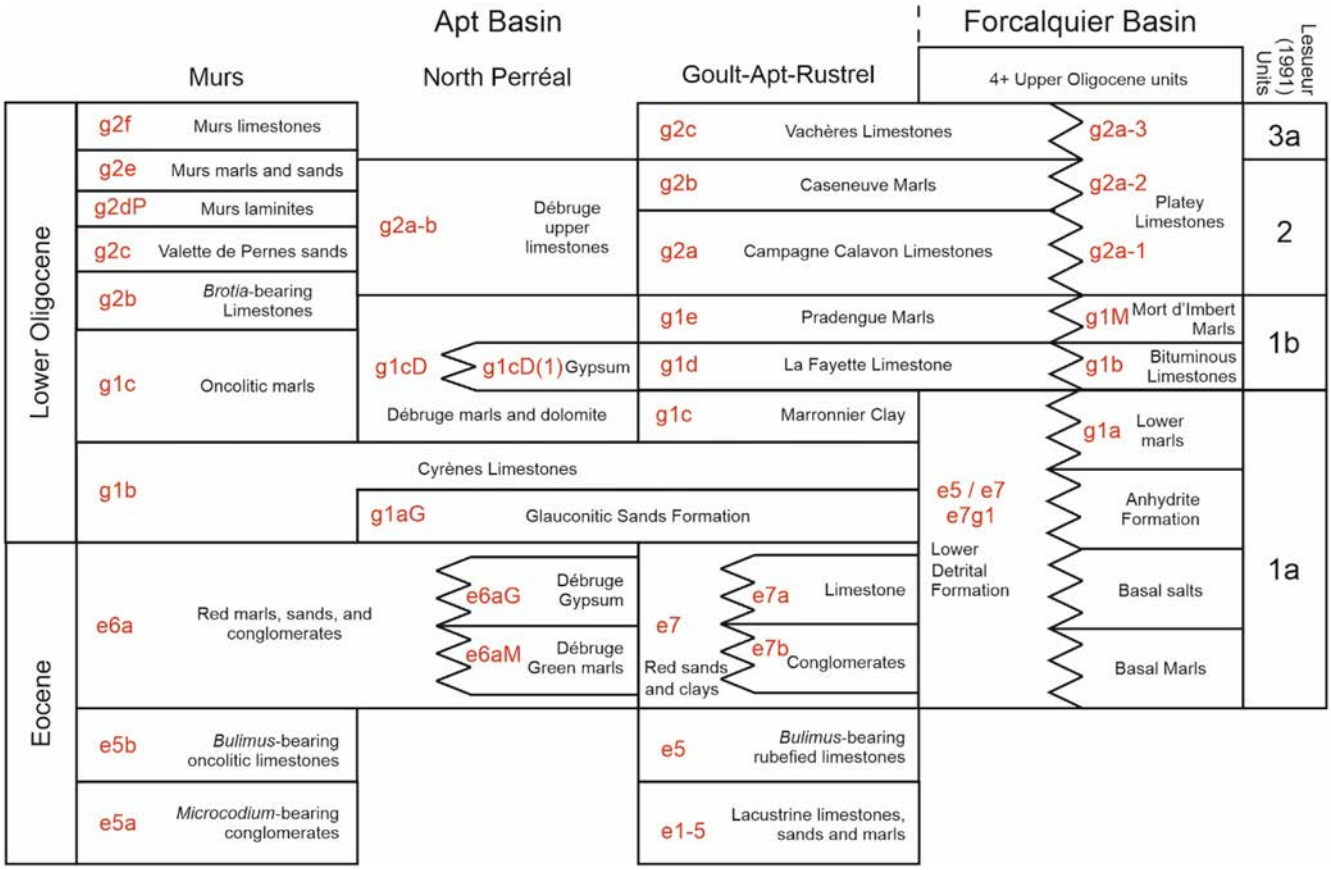

Fig. 4. Stratigraphy of the Apt Basin from the Murs and North Perréal areas (Blanc *et al.*, 1975), Goult, Apt, and Rustrel areas (Germain *et al.*, 1966; Goguel *et al.*, 1966), compared to the stratigraphy of the Forcalquier Basin (from Gigot *et al.*, 1982; Lesueur, 1991); associated coding on 1:50 000 geological maps is displayed in red. Lesueur's (1991) division of the Manosque Basin stratigraphy into sedimentological units is also displayed.

surface (*i.e.* ochreous sandstones in the northeast, Coulon Paleokarst in the south) or Urgonian limestones (in the Murs Graben).

Unfortunately, our understanding of the Cenozoic stratigraphy of the Apt Basin suffers from several inconsistencies between the different 1:50,000 geological maps that cover the area (Fig. 4). The few names of stratigraphic units that have been recurrently used in the literature are italicized and given with their French translation.

Until the deposition of the lower Oligocene *La Fayette Limestones* (*Calcaire de La Fayette* in French; g1d on Fig. 4) which are found on both sides of Flaqueirol Pass, the Apt and Forcalquier Basins host two different Eocene-lowermost Oligocene sedimentary sequences of fluvio-lacustrine deposits (grouped under sequence 1a by Lesueur, 1991). In the eastern part of the Forcalquier Basin, this sequence consists in thick deposits of salt, anhydrite and marls which reach up to 1 km of thickness near Manosque (Lesueur, 1991). Along the western and northern margin of the Forcalquier Basin, these deposits grade into fluviatile and fanglomerate deposits grouped under the *Lower Detrital Formation* (*Formation détritique Inférieure* in French; Gigot *et al.*, 1975). They are interpreted as representing a first closed-lake system centered around Manosque, with a drainage basin limited to the direct surroundings of the Forcalquier Basin, excluding the Apt Basin (Gigot *et al.*, 1975; 1977; Lesueur, 1991).

2.2.1 Eocene units

The oldest deposits of the Apt Basin are unnamed beds of reddish limestones found in the center and southern part of the basin (5 to 20 m thickness in total; e5 and e1-5 of Goult-Apt-Rustrel area on Fig. 4), interfingered with rarer beds of sands and marls. These deposits have been attributed to the lower to middle Eocene based on the presence of numerous *Romanella* casts, continental gastropods prolific in Lutetian strata of southern France (formerly known as *Bulimus* or *Amphidromus*; Plaziat, 1968). Conglomerates and sands capped by a similar layer of reddish limestones in Murs have also been attributed the lower to middle Eocene based on the presence of same fossils (e5a and e5b of Murs area on Fig. 4). Note that the stratigraphic range of *Romanella* gastropods have been later extended to the upper Eocene of the Mediterranean domain (Bensalah *et al.*, 1991). These deposits have been interpreted as representing an internally drained fluvio-lacustrine system restricted to the Apt Basin (Roch, 1971).

Later Eocene deposits are dominantly siliciclastic and most of them are unnamed and classified by lithology. East of Perréal, they consist in green marls with red paleosols and caliches, overlain by a thin bed of reddish limestone (e7 and e7a of Goult-Apt-Rustrel area on Fig. 4). These green marls yield a charophyte assemblage attributed to the Bartonian-Priabonian (Jean-Jean locality; Feist, 1977; Riveline, 1986).

The same marls yield ostracods attributed by Aspotolescu and Dellenbach (1999) to the Rupelian by comparison with ostracod assemblages of the Forcalquier Basin (Aspotolescu and Guernet, 1992). This attribution is yet to be nuanced and updated, as the Forcalquier Basin lacks Eocene ostracod assemblages for comparison. In Goult sector, the deposits are sandier and display numerous layers of conglomerates (e7b on Fig. 4). In Perréal area, these deposits comprise three lithologies: red and green sands, gypsum, and marls (e6a, e6aG and e6aM on Fig. 4). The Débruge fossil mammal bed, attributed to the Priabonian (MP18), is a lignite layer within the last meters of these deposits (Truc and Demarcq, 1967). In Murs, these deposits only consist in a few meters of green and red marls (e6a on Fig. 4). These deposits are interpreted as reflecting a later, internally drained fluvio-lacustrine system with higher siliciclastic input, centered over Perréal area where evaporites are more common (Triat and Truc, 1974; Lesueur, 1991).

In the western part of the Apt Basin, the Eocene red sand and clays are overlain by the *Glauconitic Sands Formation* (*Formation des Sables Glauconieux* in French) which thins and disappears in Perréal area (g1aG on Fig. 4). These sands are interpreted as reworked from Albian-Cenomanian glauconitic sands (Triat and Truc, 1974) and were initially attributed to the lower Oligocene based on two foraminifera taxa found at the very base of the unit, *Quinqueloculina* cf. *ludwigi* and *Rosalina douvillei* (Anglada and Truc, 1969); the age range of both taxa has more recently been extended to the upper Eocene (Barbin and Keller-Grünig, 1991). The charophyte assemblage of the same beds suggests an upper Eocene age (Feist, 1977; Riveline, 1986). The presence of foraminifera indicates a saline to brackish environment; their scarcity, lack of diversity, and the absence of any other fossil suggests a lacustrine/lagoonal environment with rare, episodic input of marine taxa (Anglada and Truc, 1969).

2.2.2 Lower Oligocene units

The *Cyrènes Limestones* (*Calcaire à Cyrènes* in French, g1b on Fig. 4) are the first geological formation unequivocally identified all over the basin. They are rich in *Cyrena* bivalves and gastropods associated with brackish environments; they include laminated and massive limestones with rarer gypsum beds and marls (Triat and Truc, 1974). Several beds yield mono-generic foraminiferal assemblages, including one bed rich in Buliminidae that recall lower Rupelian taxa from northern ECRIS basins (Anglada and Truc, 1969; Grimm, 2002; Pirkenseer *et al.*, 2010). Their lack of diversity still suggests a lacustrine/lagoonal environment with episodic connections to the sea. The development of the *Cyrènes Limestones* indicates a shallowing and decrease of the siliciclastic input into the fluvio-lacustrine system of the Apt Basin (Lesueur, 1991).

The *Cyrènes Limestones* are overlain by clay-rich beds with rarer limestones and gypsum: The *Marronnier Clay* (*argile du Marronnier* in French) in Rustrel and Apt area, *Débruge Marls* (*Marnes de la Débruge* in French) in Perréal and oncolithic marls in Murs (g1b and g1cb on Fig. 4). These beds have yielded fossil remains of *Palaeotherium* and are rich in paleosols (Goguel *et al.*, 1966). They reflect further shallowing and a renewal of the siliciclastic input into the closed lacustrine system, and represent the last episode of lacustrine sedimentation that is unique to the Apt Basin (Lesueur, 1991).

The *La Fayette Limestones* (g1d) and the subsequent *Pradengue Marls* (*Marnes de Pradengue* in French; g1e on Fig. 4) are found in both the Apt and Forcalquier Basins and overlap Flaqueirol Pass; they mark the connection of both lacustrine systems (sequence 1b of Lesueur, 1991). They grade into the *Débruge Marls* in Perréal and oncolitic marls in Murs (g1cb and g1c on Fig. 4). Thick (>10 m) gypsum beds in Perréal area (g1cb-1 on Fig. 4) indicate that the Perréal sector remained a local area of deeper waters. In the Forcalquier Basin, they grade into bituminous limestones and the *Mort d'Imbert Marls* (*Marnes de la Mort d'Imbert* in French) in Manosque area (g1b and g1M on Fig. 4, Manosque sector), also interpreted as a local lake center (Lesueur, 1991).

Three subsequent Rupelian geological units yielding occasional fossil vertebrates are found in both basins and overlap Flaqueirol Pass: the *Campagne-Calavon Limestones* (*Calcaires de Campagne Calavon* in French; dated to MP23; Helmer and Vianey-Liaud, 1970), the *Caseneuve marls* (*Marnes de Caseneuve* in French) and *Vachères Limestones* (*Calcaires de Vachères* in French; MP24; Hugueney, 1994). These units can be traced back to Perréal and Murs, where they hold different names and facies (see Fig. 4), though the exact correlation between these localities requires further work. In Murs, these deposits yield a MP23 fossil vertebrate assemblage (Rémy 2000; Costeur *et al.*, 2019). The lacustrine system later retreated to the Forcalquier Basin and Upper Oligocene deposits are only known east of Flaqueirol Pass.

3 Methods

We explored and described deposits in different places of the Apt Basin with a particular focus on the Eocene – lowermost Oligocene units below the *La Fayette Limestones* (Fig. 4). These places include nine localities displayed on Figure 3: Murs village (in the Murs Graben; MG; N43°56'26.2" E5°14'03.2"), La Rabotte farm in Roussillon (LR; 43°52'49.8"N 5°14'35.6"E), Goult village (N43°52'07.3" E5°15'33.5"), Saint Hilaire monastery in Ménerbes (SH; 43°49'23.8"N 5°15'02.5"E), La Coquillade hill in Gargas (LC; N43°52'57.0" E5°18'42.7"), the Perréal Graben in Gargas and Saint-Saturnin-lès-Apt (PG; N43°54'49.8" E5°21'25.6"), Apt city (N43°53'05.0" E5°23'02.2"), Jean-Jean hamlet in Apt (JJ; N43°54'31.2" E5°25'40.6"), and the Dog Head cliff (cirque de Pentaliane) in Caseneuve (DH; N43°54'14.9" E5°28'36.1").

We measured and logged sections at ~10 cm resolution at five localities: Murs, Goult, Perréal, Jean-Jean and Dog Head cliff. We described the sedimentary facies of these sections, classified them into 24 lithofacies adapted from the classification of Miall (2013), and grouped them into nine facies associations. Microphotographs and complementary pictures of the sedimentary facies are available in Supplementary Figures S1 and S2.

In order to provide geochronological age constraints on the deposits, eight carbonate samples from the studied localities were selected for calcite U-Pb dating; detailed geographic and stratigraphic location are given in the next section. We targeted primary micritic phases, as well as secondary (micro-)sparitic veins in order to provide minimum depositional ages.

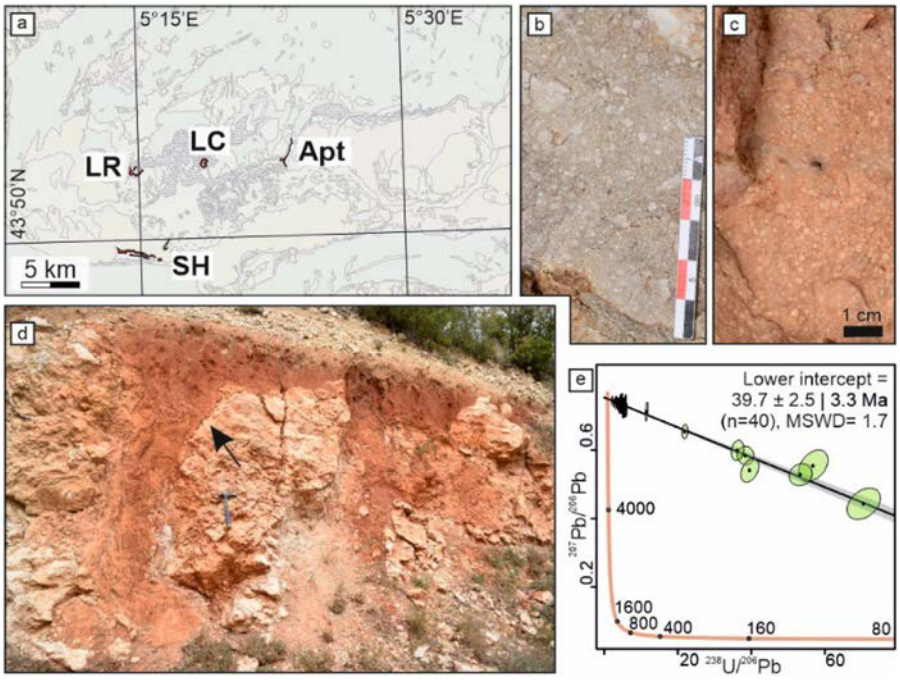

Fig. 5. (a) Location of the four localities with Eocene red limestones (LR, LC, Apt and SH) displayed on a shaded version of Figure 3 that only highlights Eocene limestones locations. LR: La Rabotte farm, LC: La Coquillade hill, SH: Saint Hilaire monastery, Apt: Apt city; (b) intraclasts in micritic mud at La Coquillade; (c) ooids at La Rabotte farm (same scale as Fig. 5b); (d) karstic surface (arrow) with cavities at La Coquillade; (e) Tera-Wasserburg diagram with isochron age of a secondary cement in a karstic cavity at La Coquillade.

U-Pb analyses were performed at the Envitop platform (CEREGE, Aix-Marseille University) on 100 μm-thick thin sections prepared at CEREGE. 40 circular spots of 150 μm diameter were picked to perform U-Pb dating after screening to maximize U-Pb variability. Calcite ablation was performed using an ESI (Electro Scientific Industries) laser (193 nm ArF Excimer laser) connected to an Element XR (Thermo Fish Scientific) Inductively coupled mass spectrometer. WC1 carbonate and NIST 614 glass reference materials were used to correct the inter-elemental fractionation. Raw data were processed with Iolite ® software and U-Pb ratios corrected for fractionation were calculated using an in-house Excel macro. Finally, U-Pb ages are calculated by using Tera-Wasserburg diagrams with IsoplotR (Vermeesch, 2018). AUG-B6 breccia was analyzed as a secondary standard to check for accuracy. It yielded an age of 42.5 ± 1.1 Ma in agreement with the age of Pagel *et al.* (2018), the uncertainty includes the propagation of the 2.5% uncertainty of the age of the WC1 primary standard by quadratic addition (Roberts *et al.*, 2017).

Further details on the methodology and the analytic parameters are given in Godeau *et al.* (2018) and their online supporting data section. Out of the eight samples analyzed for U-Pb dating, only two samples displayed enough uranium to yield a usable isochron age (Supplementary table 1). Photographs of these two samples are available in Supplementary Fig. S1.

4 Results

4.1 Eocene red limestones

The basal reddish limestones (e1-5 and e5 on Fig. 4) attributed to the Eocene crop out in four localities in the center and southern side of the Apt Basin: La Rabotte farm, Saint Hilaire monastery, La Coquillade hill, and Apt (Fig. 5a). Their exposed thickness varies from 3 m (La Coquillade) to ca. 20 m (Saint Hilaire). Their lowermost beds are only visible in Apt, where they sharply lie on weathered Cenomanian glauconitic sands. They display similar features at the four localities.

The limestones are piled up in 0.2 to 1.5 m thick beds. They are massive and rich in poorly-rounded, micritic intraclasts and oncolites isolated in a muddy micritic matrix (0.2 to 1 cm in diameter; Fig. 5b). More rarely, they can host isolated siliciclastic clasts (small quartz and sedimentary lithic sand grains and gravels). They display a varying degree of pedogenic overprint, from diffuse pinkish and reddish mottles to intense rubefaction with red root traces, which gives them their red coloration. The limestones get a nodular texture where the rubefaction is the most intense. This pedogenic overprint is the most intense at Saint Hilaire, and the least intense in Apt, where nodular layers are quasi-absent. One bed made of matrix-supported, small (<5 mm) ooids is also

observable at La Rabotte farm (Fig. 5c). Where the section is the thickest (Saint Hilaire), they alternate with rare, poorly exposed layers of massive white marls, green clays and yellowish sands. These beds yield occasional continental (*Romanella*, *Helix* and *Rillya* at La Rabotte and Saint Hilaire) and freshwater gastropods (*Planorbis* and *Limnea* in Apt; Roch, 1971).

At La Coquillade, the red limestones are overlain by a karstic surface (Fig. 5d) associated with limestone breccias, microkarst fenestrae, small karstic cavities filled up with red sands and clays from the later Eocene siliciclastic unit (e7 on Fig. 4). U-Pb dating of a secondary calcite vein (Supplementary Fig. S1a) grown in one of the cavities later filled with red sand material, yield an age of 39.7 ± 3.3 Ma (2s; Fig. 5e). This late Lutetian – early Priabonian age provides a minimum age for the development of the karstic features and a maximum age for later deposition of the red sands. Similar breccias are found in the uppermost limestone layers at La Rabotte farm directly below the late Eocene red sands, and are also found in Apt on the slopes of the outcrops, where the contact with the overlying unit is unfortunately hidden. The contact is not observable at Saint Hilaire.

A thick section of conglomerates overlain by a 2-m thick caliche in Murs was previously correlated to the Eocene red limestones based on the presence of *Romanella* gastropods in the caliche (e5a and e5b on Fig. 4, Blanc *et al.*, 1975). This section is located far to the north compared to the other limestone localities (see Fig. 3), lacks most features associated with the Eocene red limestones (quasi-absence of siliciclastic content, termination by a karstic surface), but displays sedimentary facies that can be laterally correlated with later Eocene red sands and clays (see next subsection). As noted in the geological context, later work showed that *Romanella* fossils are present throughout the early to late Eocene of the Mediterranean realm (Bensalah *et al.*, 1991). We thus argue that the lowermost deposits of the Murs Graben are lateral analogue of the later red sands and clays, and thus postdate the Eocene red limestones.

4.2 Eocene-lowermost Oligocene (?) red sands, conglomerates, glauconitic sands and gypsum

We describe here the deposits that are above the Eocene red limestones and below the *Cyrènes Limestones*; excluding the gypsum layers of the Perréal graben, they all show a prominent siliciclastic content. There are important lateral changes of sedimentary facies across the basin, but these changes are gradual and can be traced across the localities shown in Figure 6a. We split our observations into three areas: eastern sector (Dog Head cliff and Jean-Jean village; Fig. 7), Perréal Graben (Fig. 8), and the western sector (Goult and Murs; Fig. 9). Sedimentary facies and facies associations are described in Tables 1 and 2.

4.2.1 Eastern sector: green clays and glauconitic sands

Eocene siliciclastic deposits are well-exposed in the eastern sector and form quasi-continuous cliffs from Jean-Jean Hamlet up to Flaqueirol Pass (see Fig. 6a). Eocene red limestones are absent here, except in the southernmost part of the sector (near Apt). The Eocene section commonly starts with Eocene red sands, erosionally capping the ochreous Cretaceous weathering surface. These sands are sometimes ochreous or glauconitic and their color varies from white to red and green depending on their glauconite and ochre content. They are commonly massive or display trough-cross beddings that include gravel beds of chert and ferromanganese concretions (facies St). In Dog Head area, sands alternate with thinner beds of brown, pedogenised sandstones (Facies Smp; See Supplementary Fig. S2a).

At Jean-Jean section (Fig. 7), Eocene red sands laterally grade into green clays rich in pedogenic nodules (facies Fmr), forming sometimes continuous caliches (stages III and IV sensu Gile *et al.*, 1966; Fig. 6c) and two beds of reddish, bioclastic limestones (facies Clm). These two co-occurring facies form facies association FA4 (see Tab. 2 , Fig. 7). U-Pb dating of a secondary sparitic vein grown in one of the pedogenic nodules (Supplementary Fig. S1b; level 3 m, Jean-Jean section on Fig. 7) yields an age of 30.7 ± 4.7 Ma (2s; Fig. 6b). This minimum age for the development of the pedogenic nodules is compatible with the Bartonian-Priabonian age proposed for the unit.

The *Glauconitic Sands Formation* overlain the Eocene red sands and marls; in Dog Head area, the transition is gradual and both units are hard to distinguish; at Jean-Jean section, the transition is abrupt and marked by a change from marl-dominated deposits to a 60-m thick sandy sequence. Sands in the *Glauconitic Sands Formation* are less ochreous than in the Eocene red sands and marls and are prominently glauconitic. They are commonly well-sorted and are organized in laterally continuous beds that can be followed over several hundreds of meters. They display low-angle planar stratifications (facies Sp), more rarely trough cross beddings and gravels similar to the ones found in the red sands (facies St; Fig. 6d and 6e). The top of sand beds is commonly pedogenised (facies Smp) and/or overlain by pedogenised, red to brown siltstones to mudstones (facies Fmp). Pedogenic features in facies Fmp and Smp include reddish mottles and root traces and a significant increase in clay content (Bs horizons); these beds also display diffuse carbonate content, rarer slickensides and isolated pedogenic nodules, features that are common in alfisols (Retallack *et al.*, 1988).

In the last five meters of the *Glauconitic Sands Formation*, reddish mottles and carbonate content disappear and fine-grained beds Fmp beds are replaced by massive green to bleached mudstones (facies Fmr). Finally, a continuous, 20-to-100 cm thick caliche (stage IV sensu Gile *et al.*, 1966), with nodules reaching up to 15 cm in diameter, is developed in the last Smp bed (Fig. 6f and 6g; see also Supplementary Fig. S2b). This bed is incised in places and capped by a 20-to-100 cm thick bed of organic-rich, massive well-sorted sand overlain by a thin bed (1–5 cm) of lignite (facies L). Lignified roots coming down the lignite can be found in the organic-rich sand bed (see Supplementary Fig. S2c).

Co-occurring facies Sp, St, Smp, Fmp, and L form facies association FA5 (see Tab. 2, Fig. 7), which is prominent in the *Glauconitic Sands Formation*. The final lignite bed is then conformably overlain by the first limestones of the *Cyrènes Limestones*.

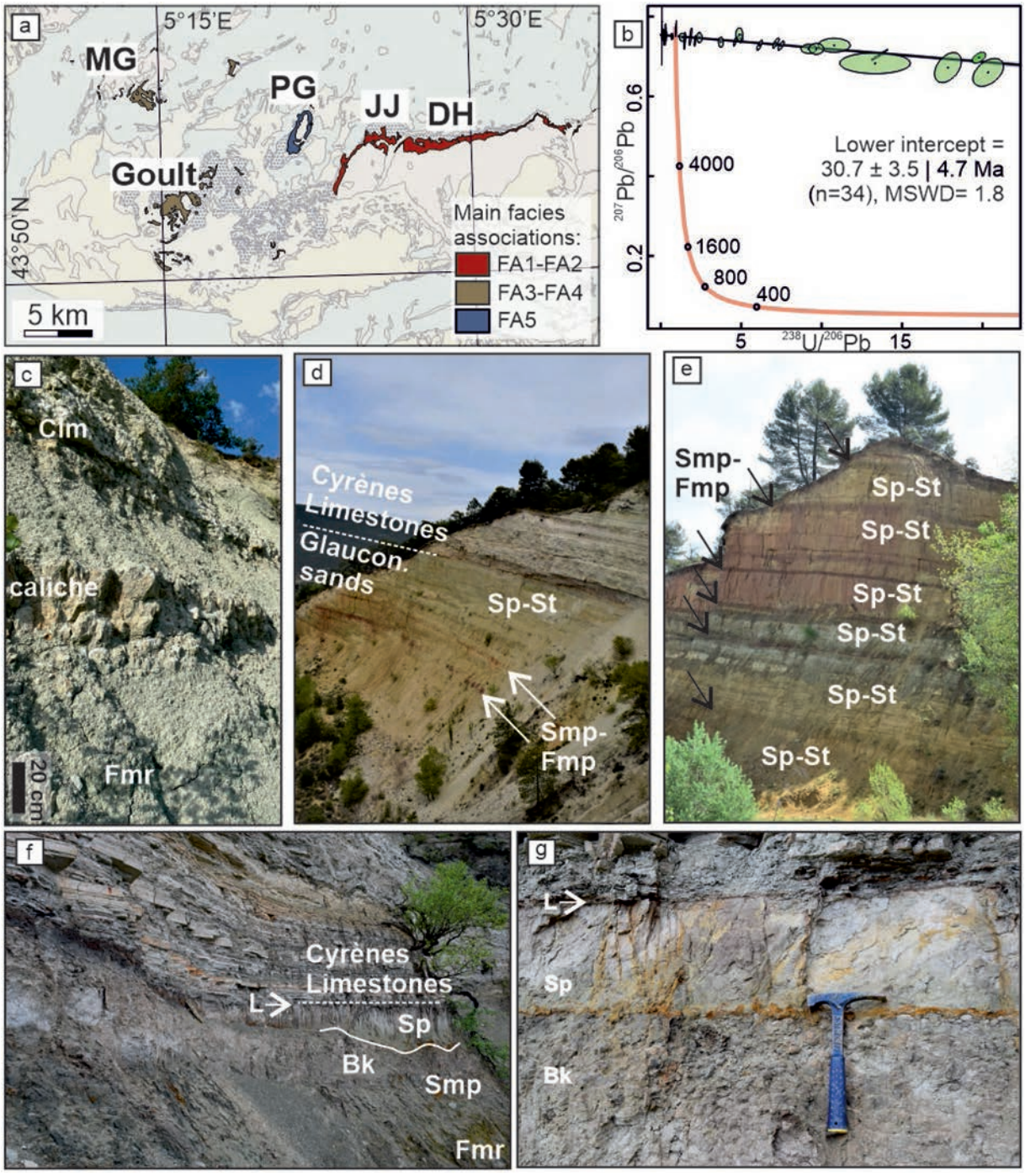

Fig. 6. **(a)** Location of the Eocene – lowermost Oligocene (?) red sands, conglomerates, glauconitic sands and gypsum on a shaded version of Figure 3, with their dominant facies association (FA; see table 2 for details). MG: Murs Graben, PG: Perréal Graben; JJ: Jean-Jean section; DG: Dog Head section. **(b)** Tera-Wasserburg diagram with isochron age of a secondary sparite in a pedogenic nodule near the base of the Jean-Jean section. **(c)** Green clays with a stage-IV caliche at the base of Jean-Jean section (facies Fmr), overlain by a bed of bioclastic limestones (facies Clm). **(d)** *Glauconitic Sands Formation* overlain by the *Cyrènes Limestones* at the Dog Head section, with regular alternations of laterally continuous, tabular beds of facies Sp-St and Smp-Fmp; trees for scale. **(e)** Regular alternations of facies Sp-St and Smp-Fmp (black arrows) at the Jean-Jean section; trees for scale. **(f)** Uppermost beds of the *Glauconitic Sands Formation* at the Jean-Jean section, showing a continuous Bk horizon overlain by an organic-rich sand bed (facies Sp; sharp erosional contact highlighted with a continuous line), overlain by a thin (<1 cm) bed of lignite (facies L); transition to the *Cyrènes Limestones* shown with a dashed line; shrub for scale. **(g)** Zoom on the last meter of the *Glauconitic sands Formation* at the Jean-Jean section, showing the Bk horizon with centimeter-sized nodules, the overlying Sp sand and the lignite L bed below the *Cyrènes Limestones*; hammer for scale.

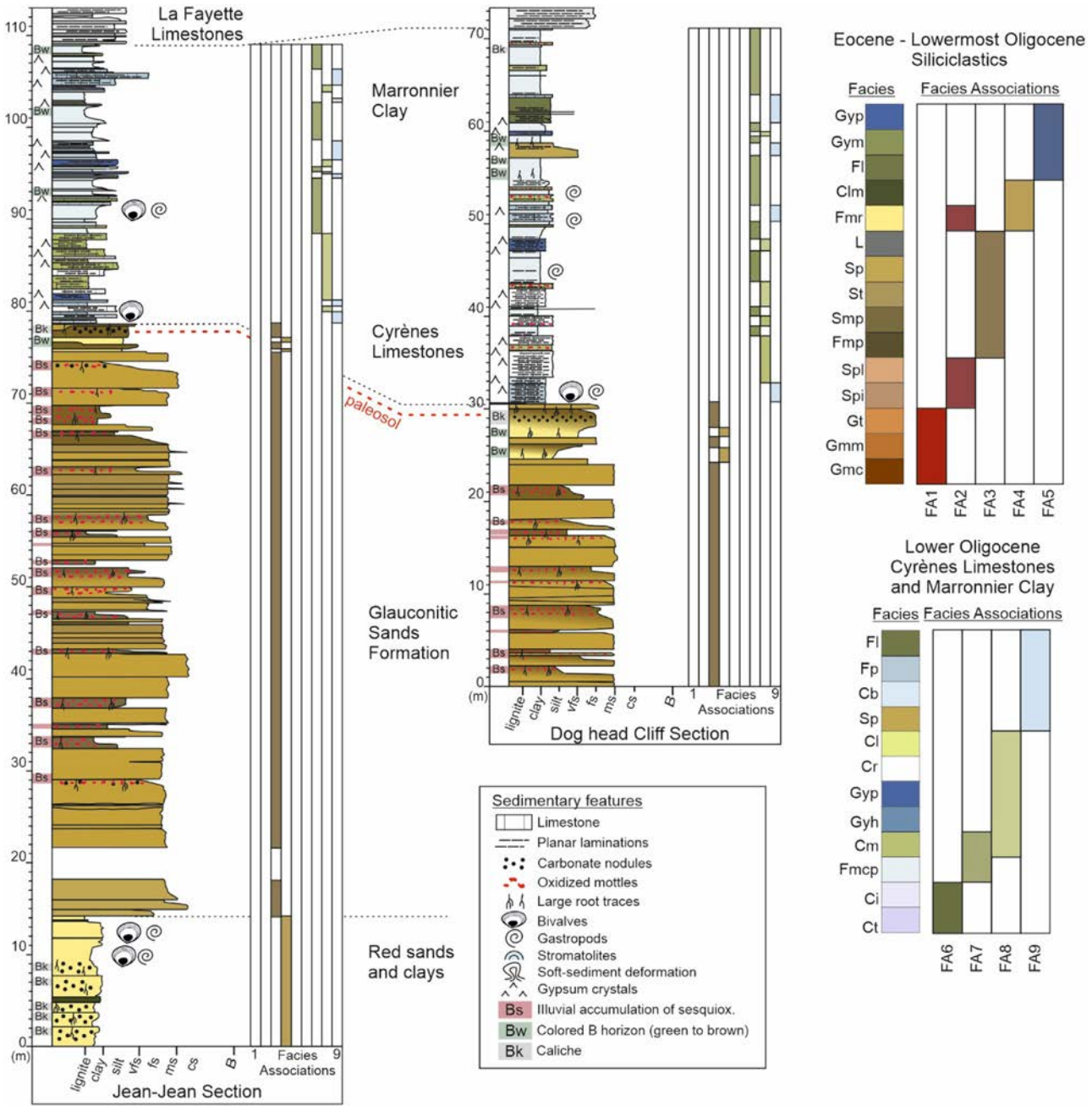

Fig. 7. Sedimentary logs at the Jean-Jean and Dog Head sections with color coding for the different facies and facies associations of the Eocene-lowermost (?) Oligocene siliciclastic deposits and the lower Oligocene *Cyrènes Limestones* and *Marronnier Clay*. The stage-IV caliche that can be found close to the top of the *Glauconitic Sands Formation* at both sections is highlighted with a red dashed line.

4.2.2 Perréal Graben: Débruge marls, gypsum and glauconitic sands

Eocene siliciclastics below the *Cyrènes Limestones* display a high lateral variability in the Perréal Graben. Eocene red limestones are here absent, and the Eocene section starts with Eocene red sands, as seen in the eastern sector. We distinguish here the southern and the western edge of the graben (Fig. 8a), where deposits crop out irregularly.

In south Perréal, the section starts with the alternation of massive red to green mudstones with rare laminations (facies Fmr), and well-sorted sands with discontinuous, slightly inclined laminations (facies Spi), more rarely wave ripple and trough cross laminations (facies Spl; Fig. 8b,c), grouped under facies association FA2 (see Tab. 2). Greenish colors and gypsum content increase up-section, first in the shape of roses, lenticular and sandy gypsum isolated in Fmr mudstones, then into continuous beds of massive, grain-supported sandy

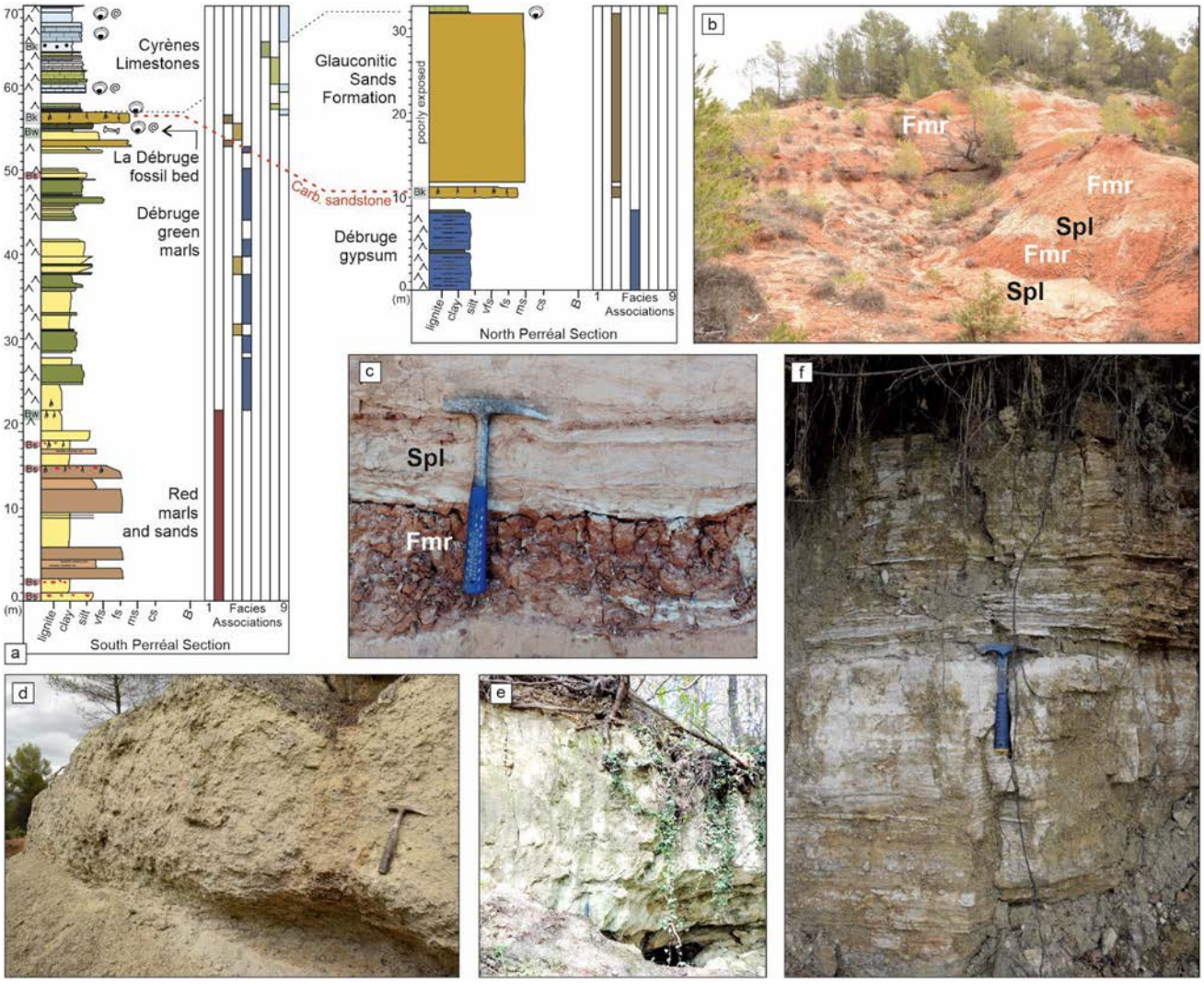

Fig. 8. **(a)** Sedimentary logs at the South Perréal and North Perréal sections (North Perréal log realized at lower, 2-m resolution). Color coding for sedimentary facies and facies associations displayed on Fig. 7. The carbonated sandstone that can be followed across the graben is highlighted with a red dashed line. **(b)** Alternations of facies Fmr (in red) and Spi (in white), south Perréal section; trees for scale. **(c)** Bed of facies Spl displaying wave-ripple and trough cross-laminations, on top of a bed of Fmr facies; south Perréal section, hammer for scale. **(d)** bed of grain-supported gypsum clasts and lenticular crystals (facies Gym), south Perréal section; hammer for scale. **(e)** Sandy limestone bed (facies Spl) on top of La Débruge fossil bed, that can be tracked all over Perréal Graben; the tunnel entrance below the limestone is a former gallery dug for the extraction of fossils; south Perréal section, hammer for scale. **(f)** Finely laminated gypsum with rarer green mudstones beds (facies Gyp), north Perréal section; hammer for scale.

gypsum (facies Gym; Fig. 8d). Beds of massive sands sometimes rich in glauconite do appear in the last five meters before the *Cyrènes Limestones* (facies association FA3). The fossil vertebrate bed of La Débruge is only found along the southeastern edge of the graben and consists of a lignite layer interfingered between Fmr facies mudstones and a *Limnae*-rich limestone (facies Cml; facies association FA4) within the last meters of sands (ca. 3 m below the *Cyrènes Limestones*). The very last meter of sands has a high carbonate content and forms a tabular bed that can be traced over the graben (Fig. 8e). The bed includes rare *Limnae,* and is rich in mottles. It gets a nodular aspect in places and big (>15 cm) rhizomorphs can also be observed. The presence of multiple well-marked pedogenic features in this bed supports a correlation with the stage IV caliche found in the eastern sector of the Apt Basin. The *Cyrènes Limestones* start on top of the tabular bed of carbonated sands.

In north Perréal, exposure is more limited but is wide enough to highlight several differences with the southern edge of the basin. The lowermost exposed beds are tabular, finely laminated beds of gypsum alternating with thin, rarer beds of green mudstones and micrite (facies Gyp; Fig. 8f), and mudstone laminites (facies Fl), grouped under facies association FA5 (see Tab. 2). Gypsum beds are then capped by the carbonated sandstone bed found all over the graben. Yet here, the carbonated sandstone is overlain by ca. 20 m of loose and massive beds of the *Glauconitic Sands Formation* (facies Sp) before the first limestone bed of the *Cyrènes Limestones* (Fig. 8a).

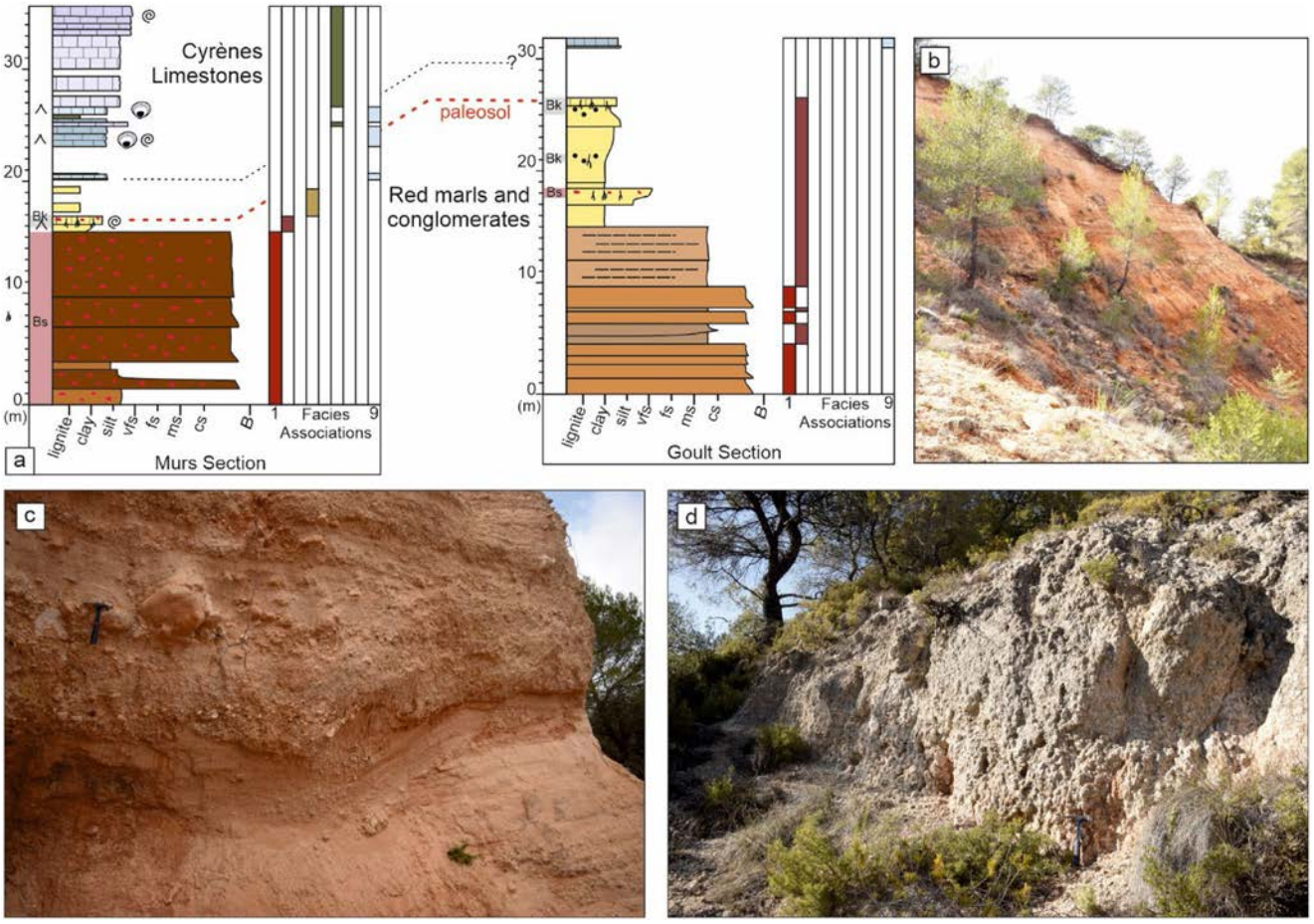

Fig. 9. (a) Sedimentary logs in Goult and the Murs Graben. Color coding for sedimentary facies and facies associations displayed on Figure 7. The stage-IV caliche that can be found close to the top of the siliciclastic deposits at both sections is highlighted with a red dashed line. (b) Alternations of facies Fmr (in red) and Spi (in white) in Goult; trees for scale. (c) bed of clast-supported conglomerates of facies Gt with erosive, channelizing base and large trough cross-beddings. (d) Caliche developed in massive, clast-supported conglomerates with normal grading in Murs (facies Gmc).

4.2.3 Western sector: red marls and carbonate conglomerates

To the west of the Perréal Graben, red marls and sands are prominent at Goult section (Fig. 9a). Well-sorted sands with planar laminations (facies Spl), more rarely with discontinuous, inclined bedding (facies Spi), and red mudstones (facies Fmr) are common throughout the section (facies association FA2; Fig. 9b). They are interfingered with 1–5 m thick bodies of clast-supported conglomerates forming trough cross-beddings (facies Gt; Fig. 9c). Clasts are almost exclusively made of Urgonian limestones, with rarer pebbles of weathered chert and iron crust. The section thins upwards and facies Fmr becomes dominant. Exposure ends with a stage-IV caliche, located ca. 5 m below the first visible bed of the *Cyrènes Limestones*.

In the Murs Graben, at the western edge of the Apt Basin, Eocene siliciclastics display a high lateral variability; sandy facies Spl, Spi, and finer-grained facies Fmr are common in places, but conglomerates of Urgonian limestone clasts make most of the exposure. Conglomerate facies are there grouped under facies association FA1 and are massive, clast-supported with normal grading (facies Gmc; Fig. 9d), more rarely matrix-supported (facies Gmm; see Supplementary Fig. S2d) or cross-bedded (facies Gt). They are mottled and commonly include *Microcodium* and pedogenic nodules. The conglomerate section ends with a 1-m thick stage-IV caliche developed in finer-grained sediment (facies Fmr), with multiple red mottles, rhizoliths and yielding *Romanella* gastropods. The paleosol is then overlain by 4 m of massive green mudstones with bare marks of pedogenesis, before the first bed of the *Cyrènes Limestones*.

4.3 Lower Oligocene Cyrènes Limestones and Marronnier Clay

Deposits from the lower Oligocene *Cyrènes Limestones* and *Marronnier Clay* are found across the basin (Fig. 10a); the same sedimentary facies are found at most sections in four facies associations (FA6 to FA9), with nonetheless a high lateral variability.

The most iconic facies of the *Cyrènes Limestones* is made of fine-grained, micritic mudstones with rarer silty layers with regular, cyclic alternations (at cm-scale) of continuous layers

Table 1. Sedimentary facies of the Eocene – lowermost Oligocene (?) siliciclastics and their interpretation. Reference for the interpretations: 1: Renaut and Gierlowski-Kordesch (2010); 2: Leeder (2016); 3: Bhattacharya (2010); 4: Miall (2010).

Facies	Grain size	Bed thickness	Description	Pedogenic features	Interpretation
Gyp	clay to medium sand	5 cm to 80 m	Beds of cm-thick continuous laminations of grain-supported, sand-sized gypsum clasts or lenticular crystals. They sometimes alternate with thin (<5 cm) beds of finely laminated green clay. Two other types of thin beds are rarely observed, interfingered within gypsum laminations: (1) <1mm-thick laminations of micritic carbonate with algal filament casts; (2) massive, fine-grained (clayey to silty) beds of micritic carbonate. The beds often display soft-deformation features (undulated bedding). Vertical burrows cross-cutting the different beds are sometimes observed, as well as fossil mammal footprints.	none	Cumulate evaporites on a low-energy, marl dominated ramp[1]
Gym	clay to medium sand	5 cm to 1 m	Beds of grain-supported gypsum clasts and crystals with a green clayey matrix (or more rarely: a carbonated silty matrix). Matrix content varies but gypsum remains dominant. Limestone intraclasts are sometimes present. Gypsum clasts are commonly sand-sized (sub-) angular grains, but bigger, euhedral prismatic or lenticular gypsum crystals are also present (see Supplementary Fig. S1c). Structure is commonly massive, rarely laminated (and deformed). They sometimes include smaller, discontinuous beds of green clays that are deformed by soft-sediment deformation.	none	Cumulate evaporites on a high-energy, marl-dominated ramp[1]
Fl	clay	1 to 5 cm	Organic-rich mudstones, with mm-thick planar laminations and rare gastropod and bivalve clasts. Sometimes rich in plant debris.	none	Lacustrine laminites[1]
Clm	mudstone to wackestone	1 to 10 cm	Sets of carbonated siltstones to silty carbonates that are either bioturbated and massive or display mm-thick laminations. Limestone intraclasts, bioclasts of gastropods and bivalves (including *Limnae*) are common, as well as plant debris. Beds are sometimes separated by thin laminations of lignite or organic-rich mud; Layers of <1 mm-thick laminations typical of microbialites are sometimes present.	rare (root traces)	Mixed marls and bioclastic deposits on a high-energy ramp[1]
Fmr	Clay to very fine sand	5 cm to 1 m	Sets of greenish/greyish (more rarely reddish) mudstones to very fine sands with a clayey matrix. Structure:	rare (fractures, mottles, root traces, and	Mixed siliciclastics on a low energy,

Table 1. (continued).

Facies	Grain size	Bed thickness	Description	Pedogenic features	Interpretation
			commonly massive, with rare, 1-5 mm-thick laminations. Limestone intraclasts, bioclasts of bivalves and gastropods and/or bioturbation (in the form of sand pockets and vertical burrows, <1 cm in length) are sometimes present. Isolated prismatic gypsum crystals or sandy gypsum in pockets are sometimes present.	pedogenic nodules)	marl-dominated ramp[1]
L	Clay	0.2 to 0.5 cm	Lignite with <1 mm-thick laminations in thin, laterally continuous (100+ m) tabular sets.	none	peat deposits[1]
Sp	fine to medium sand	10 to 50 cm thick, in cosets of 1-5 sets	Thick, laterally continuous (100+ m) of yellowish to greenish well-sorted sandstones, sometimes glauconitic. Structure consists in low-angle, 10-50 cm thick sets of massive or cm-thick planar laminations, with rarer sets of trough cross-laminations. Lenses of coarser material (coarse sand mixed with gravels or isolated boulders) occasionally occur.	Occasional presence of mottles, root traces & rhizoliths	Delta mouth bar sands[2]
St	Very fine sand to coarse sand	20 to 90 cm thick, organized in cosets of 1-5 sets	Thick, laterally continuous (100+ m) of yellowish to greenish sandstones, sometimes glauconitic. Sands are less sorted than in facies Sp. The base of the sets is sharp, often erosive, with coarser material and/or mudclasts. Structure is either massive or consists in small-scale trough cross laminations, with a coarser base. Gravels and isolated boulders occasionally occur.	Occasional presence of mottles, root traces & rhizoliths	Sand bars in delta distributary channels and mouth bar back[2]
Smp	Clay to very fine sand	Sets from 5 cm to 1 m	Dark brown to reddish grey mudstones to sandstones with clayey matrix and abundant pedogenic traces. Sets can be laterally continuous (100+ m) but sometimes thin out and disappear. Base of the sets commonly grades into underlying sandstones. Sedimentary structures come into two types: massive structure (most common), or with 1-5 mm-thick laminations and small (< 3 cm) cross-laminations that are bioturbated and discontinuous.	Common: mottles, root traces, slickensides, pedogenic nodules	channel levees[2]
Fmp	Clay to silt	5 cm to 1 m	Laterally continuous (100+ m) sets of brownish to reddish mudstones with abundant pedogenic traces. Structure is commonly massive, with rare, discontinuous 1-5 mm-thick laminations.	common: mottles, root traces, slickensides, pedogenic nodules	Overbank sheet flows in floodplain / delta plain environment[2]

Table 1. (continued).

Facies	Grain size	Bed thickness	Description	Pedogenic features	Interpretation
Spl	fine to medium sand	20 cm to 1 m	Well sorted, (cross-)laminated sands (3-10 mm thick) with rarer, slightly wavy layers of reddish mudstones (1-10 mm thick). Structure includes planar laminations, small troughs of wave-ripple and trough cross laminations, as well as rarer troughs of Urgonian limestone gravels.	Occasional presence of mottles and root traces	Sandy deltaic shoreface[3]
Spi	fine to coarse sand	50 cm to 2 m	Well-sorted sands organized in slightly inclined, discontinuous planar laminations (3-10 mm thick). Rare troughs filled with gravels and pebbles of Urgonian limestone clasts.	Occasional presence of mottles and root traces	Wave swash deposits in a beach / backshore environment[3]
Gt	Gravel to Conglomerate	50-70 cm thick, organised in cosets of 1-5 sets	Moderately sorted, clast-supported conglomerates with sandy matrix. Structure includes sets of trough cross-bedding and low angle planar stratifications, organized in fining upward cosets. The Base of each coset is sharp and erosional. Clasts are dominated by Urgonian limestones, with subordinate weathered chert, sandstone, and iron crust.	Occasional presence of mottles and root traces	Gravel bars[4]
Gmm	Conglomerate	1 to 2 m	Massive, matrix-supported conglomerates. Poorly sorted. Matrix is made of pink to red mudstones, sands, and *Microcodium*. bigger clasts are dominated by Urgonian limestone debris, with rare blocks of weathered chert.	Root traces, mottles, carbonate nodules and rhizoliths	Debris flow deposits[4]
Gmc	Conglomerate	50 cm to 5 m	Massive, clast-supported conglomerates. Faint normal grading. Clast content is similar to those of facies Gmm, though clasts are commonly bigger. The muddy to sandy matrix has a high carbonate content.	Root traces, mottles, carbonate nodules and rhizoliths	Sheet flood deposits[4]

of lenticular gypsum crystals (5 to 20 mm in size; Fig. 10b). Gypsum crystals can be so numerous that they form a crystal-supported bed within the limestones (Facies Cr; Table 3). Sets of <1 mm-thick planar laminations with algal filaments casts (facies Cl) can be spotted in places with facies Cr. Both facies sometimes display cracks filled with gypsum (Fig. 10c). Two other, gypsum-rich facies co-occur with facies Cr and Cl: facies Gyp, already observed in the Eocene gypsum deposits of the Perréal Graben (section 4.2.2), with beds of continuous laminations of grain-supported sandy and lenticular gypsum crystals (Fig. 10d), and facies Gyh, a gypsarenite displaying cross-laminations and wavy surfaces (Fig. 10e). These facies are grouped under facies association FA8 (Table 2).

Facies association FA9 first includes laminated mudstones to siltstones/wackestones rich in plant debris, with varying carbonate content and low gypsum content (facies Fp) that can yield *Cyrenae* in high concentration (Fig. 10f). They co-occur with laminites (facies Fl, already observed in the Eocene siliciclastics; see table 1), and matrix-supported limestones with intraclasts, broken *Limnae*, and other gastropods (facies Cb; Fig. 10d).

Finally, facies association FA7 consists of two co-occurring facies: massive pinkish limestones with rootlets and mottling (facies Cm; Fig. 10g), alternating with massive green to grey mudstones showing limestones intraclasts and bioclasts and pedogenic traces of varying intensity (from slickensides and vertical fractures filled with gypsum crystals to pedogenic nodules and rhizoliths; facies Fmcp).

These three facies associations occur in FA7-8-9 cycles across the *Cyrènes Limestones* and *Marronnier Clay* in the eastern sector and Perréal graben (roughly three to four cycles

Table 2. Sedimentary facies associations and their interpretation. Reference for the interpretations: 1: Leeder (2016); 2: Renaut and Gierlowski-Kordesch (2010); 3: Bhattacharya (2010).

Name	Facies	Interpretation
Eocene-lowermost Oligocene (?) deposits – siliciclastic lake system		
FA1	Gmm-Gmc-Gt	Stream-flow dominated alluvial Fan[1]
FA2	Fmr-Spl-Spi	Foreshore and upper shoreface of a coarse-grained, fluvial-dominated delta[2,3]
FA3	Smp-Sp-St-Fmp-L	Lower delta plain, mouth bar and upper shoreface of a fluvial-dominated delta[2]
FA4	Fmr-Clm	Upper shoreface of a siliciclastic lacustrine ramp margin[2]
FA5	Gym-Gyp-Fl	Lower shoreface of a siliciclastic lacustrine ramp margin[2]
Lower Oligocene *Cyrènes Limestones* and *Marronnier Clay* – saline carbonate lake system		
FA6	Ct-Ci	High-energy carbonate-dominated lacustrine shore[2]
FA7	Cm-Fmcp	Low-energy carbonate-dominated lacustrine shore[2]
FA8	Gyp-Gyh-Cr-Cm-Cl	Lacustrine ramp margin with regular drying cycles of the lake[2]
FA9	Fl-Fp-Cb-Sp	Lower shoreface of a lacustrine ramp margin[2]

at Jean-Jean and Dog Head sections, where both units are logged from bottom to top; see Fig. 7). Where logged, the *Marronnier Clay* deposits display the same facies as the *Cyrènes Limestones* with lower carbonate content and less induration. The only notable difference in the *Marronnier Clay* is the occurrence of several sets of sandstones (facies Sp) at the easternmost part of the basin (see Dog Head section, Fig. 7), the only coarse-grained siliciclastic deposits of both units.

On the opposite side of the basin, in the Murs Graben, the *Cyrènes Limestones* display slight differences. Gypsum-bearing facies are barely present and only two facies associations can be observed: the invertebrate-rich FA9 association, and the association FA6 combining two facies that are unique to the area: well-sorted sandy limestones organized in discontinuous, subhorizontal laminations (facies Ci; Fig. 10h), and sandy limestones rich in poorly-sorted bioclasts, broken oncoids and intraclasts, in small channelized bodies (facies Ct).

5 Discussion

5.1 Evolution of the depositional environments in the Apt Basin

Three lacustrine phases can be differentiated during our interval of study, separated by bounding surfaces associated with a complete drying of the lake.

5.1.1 Phase 1: Ypresian (?) – Lutetian freshwater marsh-lake system

Eocene red limestones represent a first lacustrine system occupying the southern and central parts of the basin. The most common features found in these limestones (*i.e.* numerous intraclasts and oncoids, root traces and intense oxidation) recall late Cretaceous to middle Eocene palustrine limestones of southern France (Freytet and Plaziat, 1982; Cojan and Moreau, 2006). The mixture of continental and freshwater invertebrates at some sites, as well as the persistent pedogenic overprint on limestones with a high-energy, subaqueous signature (presence of intraclasts, oncoids and oncoliths) indicate a marginal lacustrine setting experiencing frequent episodes of lake retreat and the expansion of freshwater marshes (Freytet and Plaziat, 1982; Marty and Meyer, 2006).

Eocene red limestones end with a karstic surface found at most localities, dated to the late Lutetian – early Priabonian based on the U-Pb age for a secondary sparite in a karstic depression at La Coquillade. These results indicate that this lacustrine phase likely covers the earlier times of the Lutetian and possibly extends back to the Ypresian, assuming an age no older than the Eocene for the lake system based on the regular presence of *Romanella* gastropods.

The E-W extent of the Eocene red limestones, their low siliciclastic content and limited thickness (maximum *ca.* 20 m in Apt area), and their early (?) to middle Eocene age suggest that their deposition occurred in a syn-folding depression between the Luberon and Vaucluse Range, during the Pyrenean folding of the Luberon anticline (Fig. 11a). In this regard, they recall the E-W Lutetian Eygalayes Basin, north of the Lure Mountain, formed by a combination of syn-folding subsidence and local strike-slip extension (Montenat *et al.*, 2005). Deposits of both basins are yet significantly different, with more siliciclastic input from locally exhumed faults in the Eygalayes Basin, and the alternation of marsh and playa deposits (Montenat *et al.*, 2005). A drainage connection with other known coeval basins, such as to the Eygalayes Basin in the north, to the Alpine sea to the

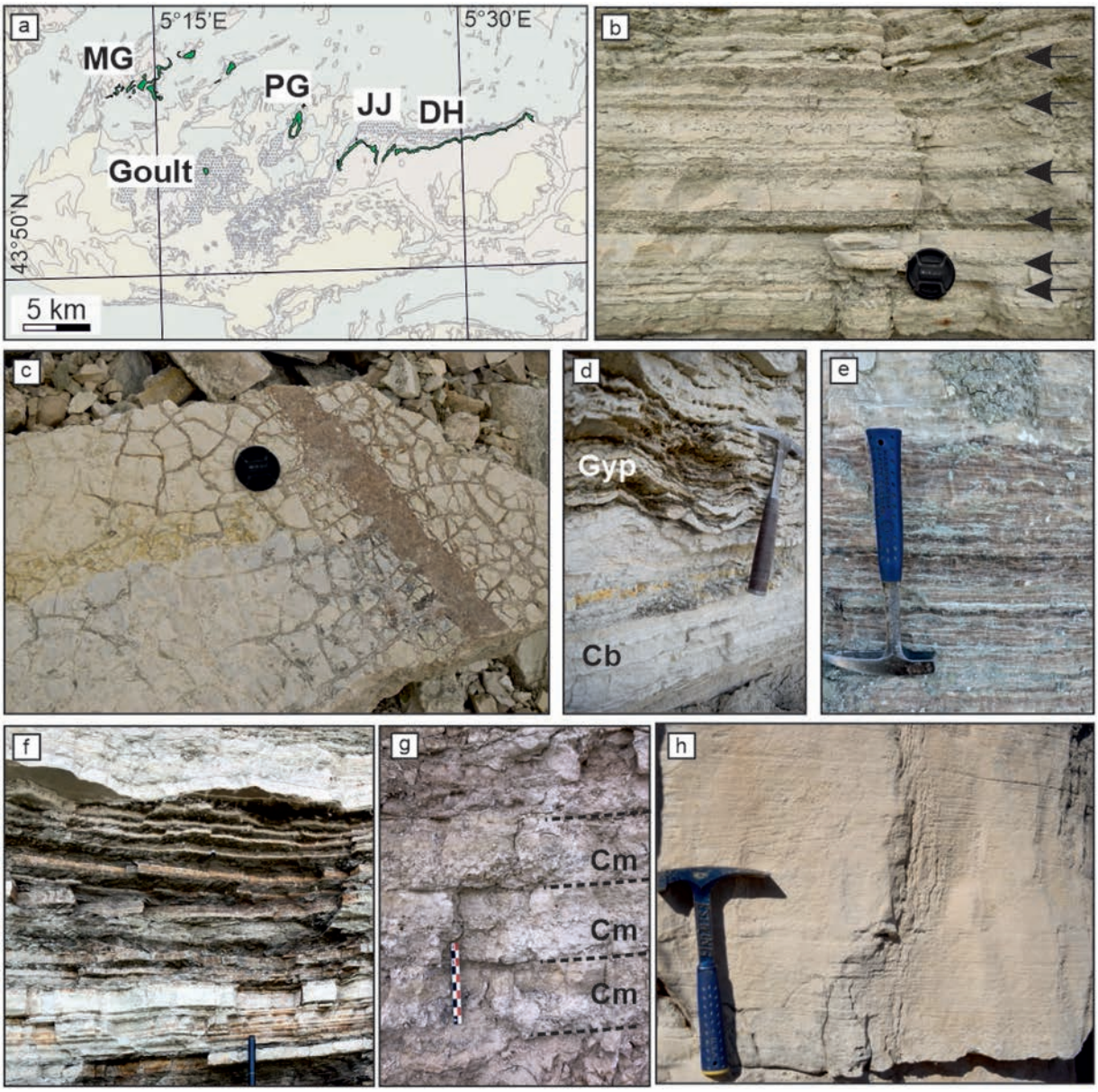

Fig. 10. (a) location of the lower Oligocene *Cyrènes Limestones* and *Marronnier Clay*, with the name of the main sections (see Fig. 6 for the caption). (b) Alternations of lenticular gypsum beds (black arrrows) and micritic mudstones in facies Cr (Dog Head section); lens cap for scale. (c) Cracks filled up with gypsum in facies Cr (Dog Head section); lens cap for scale. (d) Deformed gypsum beds (facies Gyp) on top of tabular beds of matrix-supported bioclastic and intra-clastic limestones (facies Cb), Jean-Jean section; hammer for scale. (e) Gypsarenite with cross-laminations and wavy surfaces (facies Gyh), Jean-Jean section; hammer for scale. (f) Organic-rich mudstones with varying carbonate content (facies Fp), Jean-Jean section; top of Jacob staff (10 cm) for scale. (g) Beds of massive, pink limestone (facies Cm), Jean-Jean section; scale: 10 cm. (h) Discontinuous, subhorizontal laminations in bioclastic limestone (facies Ci), Murs Graben; hammer for scale.

northeast, or to the Arc Basin to the south would require crossing several structures formed during the Pyrenean phase (Valensole High, Lure Mountain, Luberon Range, Sainte-Victoire Mountain; Sissingh, 2001; Semmani *et al.*, 2022) and thus seems unlikely. This geographical isolation, together with the evidence for important and regular lake level fluctuations, suggests a closed-basin setting for the Ypresian (?) – Lutetian freshwater marsh-lake system.

5.1.2 Phase 2: Bartonian (?) – Priabonian siliciclastic fluvio-deltaic & saline lake system

The second lacustrine phase is represented by the subsequent siliciclastic deposits found across the basin, filling-up karstic cavities developed on the Ypresian (?) – Lutetian palustrine limestones. The interpretation (Tab. 2) and distribution (Fig. 6a) of facies associations indicate a

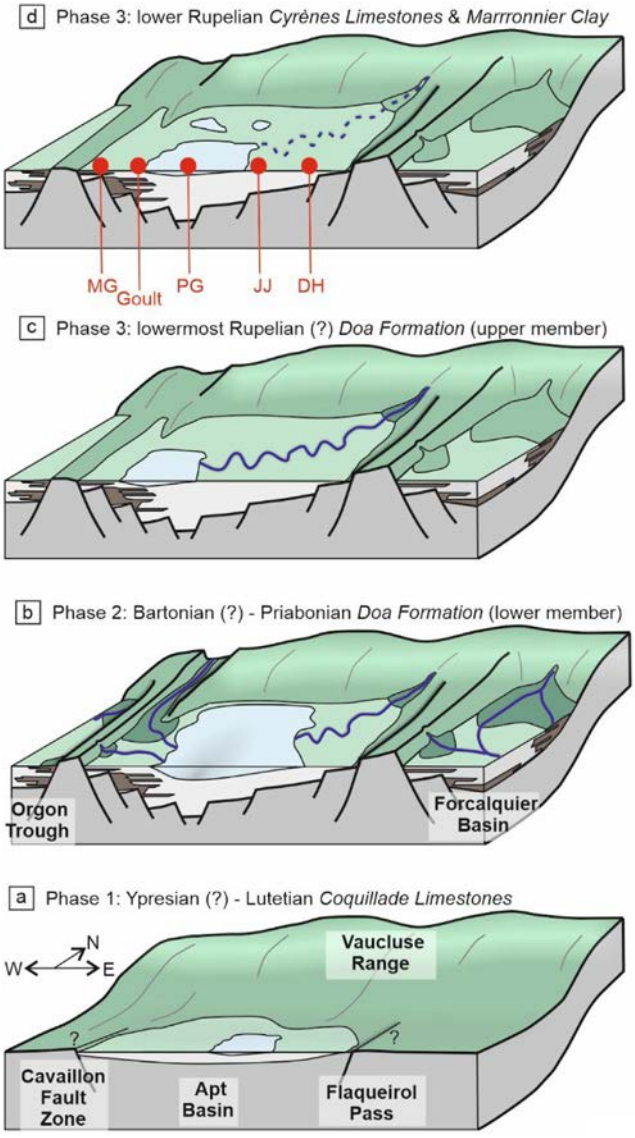

Fig. 11. Basin evolution model for the Apt Basin before its hydrological connection with the Forcalquier Basin for (a) the Ypresian (?) – Lutetian lacustrine phase, (b) the Bartonian (?) –Priabonian lacustrine phase, (c) the base of the lower Rupelian phase, and (d) the later part of the lower Rupelian phase. Location of main sections displayed on subfigure d (see Fig. 6a for caption). The *Coquillade Limestones* and *Doa Formation* are the new lithostratigraphic names introduced in Section 5.2 for the Eocene red limestones and Eocene-lowermost Oligocene (?) siliciclastic deposits. Light green color indicates areas of fluvio-lacustrine deposition, dark green color indicates area of alluvial fan deposition, intermediate green color indicates emerged areas without deposition.

prominence of fluvio-deltaic deposits in the eastern and western part of the basin, while perennial lacustrine deposits dominate in its center, in the Perréal Graben. Deltaic facies are the most widespread, and the most common lacustrine facies (FA4) are interpreted as reflecting the shallowest parts of a lacustrine ramp (Tab. 2; Renaut and Gierlowski-Kordesch; 2010). Fossil vertebrate footprints observed in the deepest facies (FA5) at North Perréal indicate that the deepest parts of the lacustrine system rarely reached more than a few meters of water level. Evaporitic deposits in FA5 indicate sustained periods with evaporation exceeding freshwater and groundwater run-off into the basin (Renaut and Gierlowski-Kordesch; 2010). They likely reflect periods of significant reduction of fluvial discharge, either on seasonal or pluri-annual scale (Renaut and Tiercelin, 1994, Larsen and Olson, 2019). Together with the presence of scarce and mono-specific foraminifera at the base of the *Glauconitic Sands Formation* (Anglada and Truc, 1969), they support a closed setting and a saline nature for this shallow lacustrine system.

In the western part of the basin, coarse-grained pedogenised facies (FA1) indicate the presence of an alluvial fan system in Murs area grading into fluvio-deltaic deposits (FA2) in Goult sector, to purely deltaic and lacustrine deposits (FA4 & FA5) in South Perréal. Conglomerate clasts are dominantly made of Urgonian limestones and associated cherts, while sands only make a minor contribution to the clastic load. These observations indicate the existence of an eastward-flowing fluvio-deltaic system, sourced west of Goult and Murs; this corroborates that the Cavaillon Fault Zone, directly west of these areas, was forming a paleo-high and that its Urgonian limestone basement was being actively eroded. In the eastern part of the basin, sandy deltaic deposits (FA3) reworked from the Albo-Cenomanian glauconitic and weathered sands dominate the sedimentary record. At our easternmost locality (Dog Head section), red and glauconitic sands dominated all thorough the section; they grade into lacustrine and deltaic plain muds (FA4 & FA5) towards Perréal Graben through Jean-Jean area. These observations indicate the existence of a second fluvio-deltaic system located at the eastern margin of the basin and recycling Cretaceous sands. They thus corroborate that the Flaqueirol Pass, directly east of these areas, was also forming a paleo-high and was the likely source of this second drainage. It remains unclear if both the eastern and western fluvio-deltaic systems were active at the same time during this lacustrine phase; deltaic facies with Urgonian limestone clasts associated to the western fluvio-deltaic system (FA2) are found at the base of the South Perréal section (Fig. 8a) and could suggest that this fluvio-deltaic system was initiated first. Collectively, the set-up of a closed lake system centered over Perréal Graben during this second lacustrine phase, associated with the erosion of both the western and eastern sides of the Apt Basin, is the first piece of evidence for E-W extension and development of the Apt basin as a graben system, bounded by actively incised horsts at the location of the Cavaillon Fault zone and Flaqueirol Pass (Fig. 11b).

The onset of the second lacustrine phase must postdate the 39.7 ± 3.3 Ma (2s) age constraint for the karst development in La Coquillade but predate the middle Priabonian, age of the Débruge vertebrate fossil locality, occurring at the very top of the siliciclastic succession in South Perréal, and the early Oligocene U-Pb age found in a secondary calcite at the base of the Jean-Jean section. Our field investigations have highlighted the presence of a basin-wide limestone bed in the uppermost meters of these siliciclastic deposits below the *Cyrènes Limestones*. On the basin margins (western and eastern sector), this bed is identified as a caliche. In the center of the basin (Perréal Graben), the presence of *Limnae* together with the pedogenic features rather suggests a palustrine nature for the

limestone. This surface indicates a complete retreat and drying of the lake, up to a final marsh in the Perréal Graben, and thus the end of this lacustrine phase. The Débruge fossil horizon is located just below the limestone bed, indicating a middle to late Priabonian age for the end of the siliciclastic fluvial-lake system. The age of the second lacustrine phase can thus be attributed to the Bartonian (?) – Priabonian. The end of this lacustrine phase could be synchronous with the Eocene-Oligocene Transition, though more precise dating of these strata is required to test this hypothesis. At the South Perréal section (Fig. 8a), evaporitic deposits become prominent for 30 m before disappearing 3 m below the uppermost palustrine limestone bed. They suggest an earlier decrease of seasonal fluvial discharge and/or an increase in the frequency of pluriannual arid events, that could have paved the way to the complete retreat of the lake.

5.1.3 Phase 3: lower Rupelian saline carbonate lake system

The ca. 20 m of deltaic sands (FA3) on top of the carbonated sandstone bounding surface in North Perréal (Fig. 8a) mark the onset of a new depositional phase in the basin. The same deltaic sands can be tracked in the eastern part of the basin, where they are significantly thin (<1 m thickness), incise the bounding surface (Fig. 6f), and are associated with the development of an histosol (overlying lignite). Siliciclastic deposits on top of the bounding surface in the western part of the basin are finer-grained (Fig. 9a) and attributed to a lacustrine upper shoreface environment (FA4). Taken together, this facies distribution indicates a renewal of siliciclastic input from the eastern part of the basin (erosion of Cretaceous sands from the Flaqueirol Pass area) and the beginning of a third lacustrine phase, in a context of continued subsidence in the northern part of the Perréal Graben. The finest-grained and most distal lacustrine facies (FA4) seem to have shifted towards the western part of the basin, indicating the complete shut-down of coarse sediment input in the eastward-flowing fluvio-deltaic system sourced in the Cavaillon Fault Zone (Fig. 11c).

The renewal of siliciclastic input seems to be short-lived as these sand- and mud-dominated facies conformably shift to the carbonate-dominated lacustrine facies of the *Cyrènes Limestones* and *Marronnier Clay* basin-wide. The dominant facies associations of the third lacustrine phase (FA7, FA8, and FA9) form a gradual transition along the ramp of a perennial, saline lacustrine system dominated by carbonate production and evaporite accumulation (Tab. 2; Renaut and Gierlowski-Kordesch; 2010). Three observations indicate a gentle nature for the lacustrine slope and the absence of a significant depth (> a few m) in the lake system: (1) the presence of the three facies associations at most localities, with no clear location with higher occurrence of deeper facies; (2) desiccation marks even the deepest carbonate facies (Cb; Table 3); (3) very regular vertical and horizontal shifts from a facies association to another, suggesting that they reflect only subtle depth variations. The regular carbonate-gypsum cycles (cm-scale, facies Cr) found at most places indicate the regular alternation of flooding and evaporation in the lake system (Leeder, 2016), generating small lake level fluctuations. FA7-8-9 cycles seen at the scale of several meters at the Jean-Jean and Dog Head sections indicate lake level changes at longer time scale and greater depth range. These features indicate the persisting closed nature of the lake system. Together with the presence of scarce and poorly diverse foraminifera in the *Cyrènes Limestones* (Anglada and Truc, 1969), they support a saline nature of this shallow lacustrine system, such as seen for phase 2.

Beach and bioclastic sand bar deposits without any siliciclastic content (facies Ct and Ci; FA6 in Table 2) in the Murs Graben confirm the complete shut-down of siliciclastic input from the Cavaillon Fault zone during the third lacustrine phase. They represent marginal lacustrine conditions that indicates that the area remained at the edge of the lacustrine basin. The high energy of these facies (Renaut and Gierlowski-Kordesch; 2010) contrasts with other marginal lacustrine facies found in the basin (FA7). Indeed, bioclastic sand bars indicate an environment with higher flow, which could indicate episodical freshwater input from the eastward-flowing freshwater drainage identified during phase 2, or episodical water connections with neighboring basins. At the other edge of the basin, to the east, the occurrence of deltaic sandstones (facies Sp) in the *Marronnier Clay* at Dog Head section indicates ephemeral reactivations of the eastward-flowing fluvial system flowing from the Flaqueirol Pass area (Fig. 11d).

The onset of the third lacustrine phase must postdate the middle Priabonian (age of the Débruge Fauna). The development of a markedly pedogenised surface at the end of the second lacustrine phase indicates a prolonged time of sedimentary quiescence before the onset of the third phase; it is thus likely that the uppermost part of the Eocene is missing in the Apt Basin. There is no biostratigraphic age constraint for the basal siliciclastic deposits at the base of the third lacustrine phase, but the *Cyrènes limestones* are attributed to the lower Rupelian based on their foraminifera assemblage (Anglada and Truc, 1969). We thus attribute the beginning of the third phase to the lower Rupelian. The third phase ends with the beginning of the *La Fayette Limestones* that are found on both sides of Flaqueirol Pass, including on the pass, and the connection of the Apt Basin with the neighboring Forcalquier Basin. The transition to the *La Fayette Limestones*, where logged (Jean-Jean and Dog Head sections; Fig. 7) is conformable and associated with sand beds showing wave ripples, flaser and lenticular bedding (not shown). The age for the end of the third phase is constrained by the MP23-24 land mammal ages of fossil localities found above the *Marronnier Clay*, in the Murs Graben and Forcalquier Basin (Ménouret, 2014). The third lacustrine phase would thus have ended around 30 Ma.

5.2 A new chronostratigraphic framework for the Apt Basin

The late identification of three lacustrine phases in the Apt Basin, despite extensive previous work, is mainly due to the intricate stratigraphy of the basin and its location at the edge of three geological maps (Fig. 4). We propose to simplify this framework by grouping some of the deposits described here into two lithostratigraphic units that aim to simplify further mapping, paleontological and sedimentological work in the Apt Basin (Fig. 12):

-The *Coquillade Limestones* (*Calcaires de la Coquillade* in French) group the Eocene red limestones of La Coquillade,

Table 3. Sedimentary facies of the lower Oligocene *Cyrènes Limestones* and *Marronnier Clay* and their interpretation. (*) indicates facies also present in Eocene − lowermost Oligocene (?) deposits (Table 1). Reference for the interpretations: 1: Freytet and Plaziat (1982); 2: Renaut and Gierlowski-Kordesch (2010); 3: Leeder (2016); 4: Bhattacharya (2010); 5: Miall (2010).

Facies	Grain size	Bed thickness	Description	Pedogenic features	Interpretation
Cl	mudstone	1 to 20 cm	Sets of <1 mm-thick planar laminations. Surfaces are planar, rarely undulated, with algal filament casts.	Rare (mud cracks filled-up with gypsum).	Microbialite[1]
Fl (*)	mudstone to siltstone	1 to 5 cm	See table 1 for a full description.	none	Lacustrine laminites[2]
Fp	mudstone to siltstone	1 to 10 cm	Mudstones to siltstones/wackestones rich in plant debris, with varying carbonate content. Structure is commonly laminated (with 1-5 mm-tick laminations; see Supplementary Fig. S1d), more rarely massive. Sets of changing grain-size and organic content alternate at pluricentimeter to centimeter frequency. Differs from facies Clm (table 1) on two points: (1) Complete bivalve (cyrenae) molds in high concentration can be found within sets or at set boundaries; (2) Lenticular gypsum is rare, but is sometimes present in continuous layers.	none	Mixed marls and bioclastic deposits on a high-energy ramp (lower shoreface)[2]
Cb	mudstone to wackestone	5 to 20 cm	Matrix-supported limestone with a micritic, clayey to sandy matrix. Structure is commonly massive, more rarely with mm-thick laminations. Carbonate intraclasts, broken clasts of gastropods (including *Limnae*) and bivalves are common. Vertical and horizontal burrows can occur, as well as lenticular gypsum (though less repetitively than in facies Cr).	Rare (mud cracks filled-up with gypsum).	Mixed marls and bioclastic deposits on a high-energy ramp (upper shoreface)[2]
Sp (*)	Very fine to medium sand	5 to 20 cm thick	See table 1 for a full description.	none	Delta mouth bar sands[3]
Cr	mudstone	1 to 10 cm	Sets of fine-grained, micritic limestones with rarer silty layers. Structure is either laminated (with 1-5 mm-thick laminations) or massive. They sometimes include charophytes, but they are otherwise abiotic. The facies is characterized by regular alternations (at the scale of several centimeters) of continuous layers of lenticular gypsum crystals (1 to 20 mm in size; see Supplementary Fig. S1e). Gypsum crystals are matrix-supported or can be so numerous that they form a crystal-supported bed within the limestones.	rare (mud cracks filled-up with gypsum).	Flood deposits −evaporative cycles on a high-energy ramp (upper shoreface)[3]
Gyp (*)	clay to medium sand	5 cm to 80 m	See table 1 for a full description.	none	Cumulate evaporites in perennial saline lake[2]
Gyh	Siltstone to medium sand	2-5 cm	Small sets (2-5 cm) of gypsum sands with cross-laminations and wavy surfaces. Cosets can form thick benches of indurated gypsum. Discontinuous sets of carbonated siltstones are sometimes present, with wavy surfaces, forming a heterolithic flaser bedding. Flame structures and soft-deformation features (undulated bedding) are common.	none	Reworked evaporites on a high energy lacustrine ramp (upper shoreface)[2]
Cm	Mudstone	20 cm to 50 cm	Pink to white, massive limestones with a silty to sandy micritic matrix. They are sometimes	Common: small rootlets.	Palustrine marsh deposits[1,2]

Table 3. (continued).

Facies	Grain size	Bed thickness	Description	Pedogenic features	Interpretation
			gypsiferous (with grain-supported to matrix supported gypsum sands) with Occasional cavities and vugs (see Supplementary Fig. S1f). They often display tiny (<1 cm long) rootlets that are either oxidized or filled with green clay. The base and thickness of sets are irregular; they laterally grade into facies Cr or Cb.		
Fmcp	Mudstone	5 cm to 1 m	Sets of green, blue to greyish (more rarely light brown) massive mudstones with variable carbonate content. Carbonate intraclasts and broken pieces of tuffa are sometimes present, as well as horizontal burrows filled-up with silt or gypsum sands.	Occasionally present: mottles, slickensides, vertical fractures (sometimes with gypsum), pedogenic nodules, rhizoliths and root traces	Marls on a low-energy ramp (upper shoreface)[2]
Ci	fine sand	20-70 cm thick	Well-sorted sandy limestones organized in discontinuous, subhorizontal laminations. Structure also includes rare troughs of cross laminations (1 cm thick) and troughs of bigger (1-5 mm) bioclasts.	None	Wave swash deposits in a bioclastic beach / backshore environment[4]
Ct	very fine to coarse sand	15 to 50 cm thick	Sandy limestone rich in poorly-sorted bioclasts, broken oncoids and intraclasts, in small channelized bodies (meter-wide). Sets have a sharp base and are fining upward. Structure is either massive or displays small troughs (1-5 cm) of cross laminations.	None	Bioclastic sand bar[5]

Saint Hilaire, Goult and Apt (units e5 and e1-5 on Fig. 4; see Sect. 4.1). They are named after the site of La Coquillade, where the age of their final karstification has been dated. Our work shows that their age is Ypresian (?) – Lutetian.

- -The *Doa Formation* (*Formation de la Doa* in French) groups all the siliciclastic and evaporitic deposits between the *Coquillade Limestones* and the *Cyrènes Limestones*. It is named after the Doa River draining the eastern part of the Apt Basin and generating great exposure of these deposits (Jean-Jean and Dog Head sections). The *Doa Formation* is divided into a lower and upper members by the pedogenised bounding surface marking the transition between the second and third lacustrine phase (Fig. 11 and 12). The lower member makes most of the thickness of the Doa Formation and is attributed to the Bartonian (?) – Priabonian; it covers the entire second lacustrine phase and the Débruge fossil fauna. The upper member is only a few meters thin but in North Perréal, and cover the base of the third lacustrine phase. It is attributed to the lowermost Rupelian, pending further dating.

5.3 Tectonic and climate history of the Apt Basin

The existence of three lacustrine phases with markedly different features provides unusual insights into the complex regional tectonic and climatic evolution of the region between the middle Eocene and the early Oligocene.

We showed that the first and second lacustrine phases likely respond to different subsidence mechanisms: Pyrenean syn-folding for the Ypresian (?) – Lutetian phase, E-W extension and graben formation for the Bartonian (?) – Priabonian phase. Our work dates the end of Pyrenean deformation in Provence to the latest Lutetian – Bartonian, shortly followed by the onset of ECRIS rifting and extension in the Bartonian (?) – Priabonian. We see no clear change of deformation that could explain the end of the second lacustrine phase; graben-style subsidence seems to outlive the period of sedimentary quiescence at the end of phase 2, as witnessed by the thickness of the glauconitic sands on top of the palustrine limestones (upper member of the *Doa Formation*) in North Perréal. The change of lacustrine sedimentation style between phase 2 and phase 3, as well as the likely synchronicity of the end of phase 2 with the Eocene-Oligocene Transition, suggest that climate changes could be driving this transition.

Indeed, the different sedimentological features of the three lacustrine phases indicate an overall increase of aridity through time in the area. The recurrence of palustrine facies suggests a sub-humid climate during the first lacustrine phase, and the absence of evaporitic minerals, despite the possibly closed nature of the basin, corroborates a relatively high humidity at the time of deposition (Alonso-Zarza, 2003). The appearance of thick evaporites in the deeper lacustrine facies and recurring caliches in the most on-shore parts of the second lacustrine phase indicate a shift to a seasonally dry environment with marked seasonal aridity and/or regular pluri-annual arid events (Renaut and Gierlowski-Kordesch, 2010). The final, complete dry-out of the lake ending of phase 2 is interestingly not

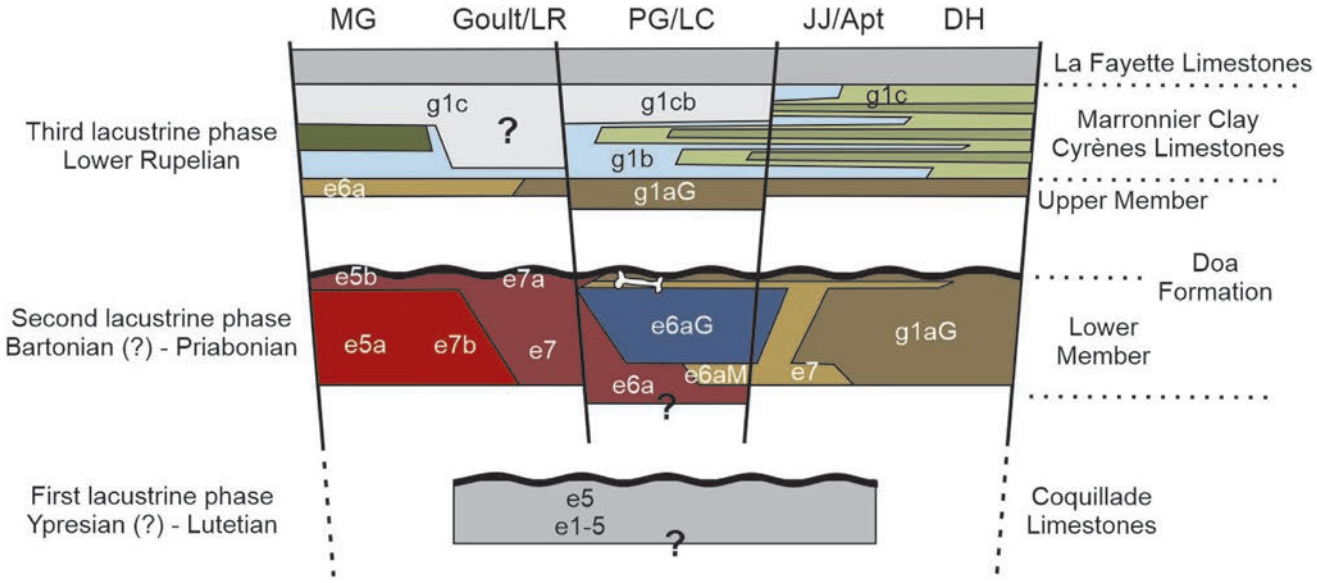

Fig. 12. Proposed chronostratigraphic framework for the Apt Basin deposits before its connection with the Forcalquier Basin across the studied sections (See Fig. 5a and 6a for their complete name and location). Color coding corresponds to facies associations of Fig. 7. Dark grey color corresponds to facies that were not described, light grey color to deposits that were not observed in the field. The mapping code of previous units from Fig. 4 is also displayed with their chronostratigraphic position. The white bone corresponds to the stratigraphic location of the Débruge fossil bed.

associated with evaporitic deposits, unlike what is seen during late Eocene drying events in the Alès Basin (Letteron *et al.*, 2022), but the set-up of marsh conditions at the center of the basin. We thus suggest that this lake retreat is associated with both a decrease of run-off and evaporation, to ensure a positive balance between run-off and evaporation during the lake retreat. A combination of regional cooling and decrease of precipitation, as seen in other regions through the Eocene-Oligocene Transition (Page *et al.*, 2019; Toumoulin *et al.*, 2022), could explain these features. After a short phase of re-watering associated with a siliciclastic impulse, the third lacustrine phase was dominated by biochemical processes and carbonate deposition with a quasi-absence of siliciclastic input. Widespread carbonate sedimentation during this phase was likely enhanced by the prominently carbonated (Urgonian) nature of the basement in the drainage area (Gierlowski-Kordesch, 1998). The decrease of siliciclastic input nonetheless suggests that the third phase was characterized by more limited surface water runoff than the previous phases. The sedimentary facies of the third lacustrine phase recall closed semi-arid lakes of the American Southwest (Leeder, 2016). The presence of regular gypsum-limestone couplets (facies Cr), mudcracks and other pieces of evidence for seasonal lake retreat and aerial exposure in the *Cyrènes Limestones* suggest that this lake system might have occasionally looked like a wide playa-mud flat system with perennial saline waters seasonally limited to a few ponds in the center and western parts of the basin.

5.4 Implications for the connectivity and paleogeography of the ECRIS system

Our study highlights the persistence of closed-basin setting for the Apt Basin from the Ypresian (?) – Lutetian to the lower Rupelian. Prominent palustrine facies and the lack of siliciclastic input during the Lutetian indicate a lack of topography at the edges of the basin; they corroborate previous studies proposing that the topography associated with regional Pyrenean anticlines and thrusts significantly postdate the Pyrenean orogeny and rather reflect post-Burdigalian Alpine deformation (Ford and Stahel, 1995; Clauzon *et al.*, 2011).

In contrast, evidence for siliciclastic input, alluvial fan and fluvio-deltaic systems during the Bartonian (?) –Priabonian highlights the presence of topographic highs at the location of the Cavaillon Fault zone and Flaqueirol Pass, making any connection with neighboring basins (Mormoiron, Orgon and Forcalquier Basins) unlikely. The presence of evaporites and rare foraminifera during the second lacustrine phase cannot thus be explained by ephemeral connections to seawater via the neighboring basins (Semmani *et al.*, 2023). Gypsum is commonly present as crusts and isolated crystals in the Cretaceous Coulon Paleokarst, as a result of pyrite weathering during the karstification process (Guendon and Parron, 1983). We suggest that the dissolution (and later reprecipitation) of this gypsum during the Eocene incision of the Cretaceous weathering surface could be the source of the Apt Basin evaporites. We showed that topography along the Cavaillon Fault zone was likely significantly reduced by the third lacustrine phase; this reduction leaves the door open for ephemeral sea incursions into the Apt Basin from the west, either from the Mormoiron Basin or the Orgon Trough, starting from *Cyrènes Limestones* times. High energy carbonate facies in the Murs Graben could have witnessed such ephemeral through-flows; these episodes remain to be clearly shown by further sedimentological or geochemical studies.

Our work confirm that the Forcalquier Basin remained completely isolated from the Apt Basin until the *La Fayette Limestones* (middle Rupelian), which raises the question of the origin of the thick salt deposits found there at the base of the

Paleogene sequence. Most of the salts found in the Forcalquier Basin predate the *La Fayette Limestones* (Fig. 4), and thus the connection to the Apt Basin. If these salts are marine in origin, the only possible sea connection has to be looked for to the southeast, through the Ryans and Salerne synclines (Semmani *et al.*, 2023).

6 Conclusion

Our sedimentological and geochronological investigations show that the Eocene-lower Oligocene stratigraphic record of the Apt Basin can be divided into three lacustrine phases before its final connection to the neighboring Forcalquier Basin, each separated by complete drying episodes:

- A first phase dominated by palustrine limestones (named here the *Coquillade Limestones*), dated to the Ypresian (?) – Lutetian and corresponding to syn-folding sedimentation during the latest part of the Pyrenean orogeny;
- A second phase dominated by siliciclastic sediments and evaporites (lower member of the *Doa Formation*), dated to the Bartonian (?) – Priabonian and corresponding to the onset of E-W extension and the development of the Manosque graben system;
- A third phase, first marked by a short siliciclastic impulse (upper member of the *Doa Formation*) and followed by carbonate production and evaporite deposition (*Cyrènes Limestones* and *Marronnier Clay*), dated to the lower Rupelian. Complete drying of the second lacustrine phase and the subsequent onset of the third lacustrine phase dominated by biochemical processes possibly represent the regional environmental response to cooling and drying across the Eocene-Oligocene Transition.

The facies distribution and location of Eocene sediment distributary systems exclude any connection between the Apt Basin and other neighboring basins, indicating a local origin for the evaporites. Ephemeral sea incursions into the Apt Basin become plausible during the lower Rupelian, when the topography at the western edge of the basin is apparently removed. We show that the Forcalquier Basin remained fully isolated from the Apt Basin until the middle Rupelian (*La Fayette Limestones*), raising questions about the potential marine origin of its evaporites.

Supplementary materials

Supplementary Table 1: Carbonate U-Pb data

Supplementary Figure S1: (a) Slide of the limestone from La Coquillade that was analyzed for U-Pb dating, showing the red, microsparitic secondary vein that was targeted (black arrow). **(b)** Slide of the pedogenic nodule from Jean-Jean section that was analyzed for U-Pb dating, showing the sparitic vein that was targeted (black arrow). **(c)** Microphotograph in non-polarized light of facies Gym, Dog Head section, showing grain-supported gypsum clasts and lenticular crystals. **(d)** Microphotograph in non-polarized light of facies Fp, Dog Head section, showing laminations and flat-lying bivalve shells. **(e)** Microphotograph in non-polarized light of facies Cr, Dog Head section, focused on a bed of lenticular gypsum crystals. **(f)** Microphotograph in non-polarized light of facies Cm, Dog Head section, showing massive micrite with isolated gypsum vugs, oxidation and dissolution marks.

Supplementary Figure S2: (a) Mottles and small carbonate nodules in facies Smp, Dog Head section. **(b)** Pedogenic nodules in the paleosol at the top of the Eocene siliclastic sequence (second lacustrine phase) forming a continuous, tabular horizon (stage-IV caliche), Dog Head section. **(c)** Organic-rich sands below a lignite bed at the base of the third lacustrine phase, Jean-Jean section. **(d)** Picture of facies Gmm and Gmc near Murs. Gmm facies is matrix-supported with a light red sandy, Microcodium-bearing matrix, while facies Gmc is clast-supported with a micritic matrix.

The Supplementary Material is available at https://www.bsgf.fr/10.1051/bsgf/2024019/olm.

Acknowledgments

This research was primarily funded by the French Research Agency ANR grant ANR-19-ERC7-0007 and European Research Council (ERC) under the European Union's Horizon 2020 research and innovation program (grant agreement No. 101043268). We thank J. Longerey and F. Demory for their assistance in the lab; Mme Ughetto, N. Meijer, G. Dupont-Nivet, A. Boura, A. Tosal, A. Nutz and S. Legal for their assistance in the field. We also thank the Fruchart-Chemery family, the Parc Naturel Régional du Luberon, the Bussat family and the team of Les Valseuses for hosting us multiple times during our field trips. AL does not thank the inhabitant of Murs who punctured his tire while he was logging in the field. CEREGE Envitop analytical facility received support from the "Excellence Initiative" of Aix Marseille University A*MIDEX – project DATCARB, a french "Investissement d'avenir" program. The authors have no conflict of interest to declare.

Data availability statement

The data that supports the findings of this study are available in the supplementary material of this article.

References

Alonso-Zarza AM. 2003. Palaeoenvironmental significance of palustrine carbonates and calcretes in the geological record. *Earth-Sci Rev* 60: 261–298.

Anglada R, Truc G. 1969. Présence de foraminifères dans l'Oligocène inférieur du synclinal d'Apt (Vaucluse, Sud-Est de la France); conséquences paléo-écologiques et paléogéographiques. *CR Acad Sci Paris Ser D* 269: 312–315.

Apostolescu V, Guernet C. 1992. Les ostracodes oligocènes de la région Forcalquier-Manosque (Bassin continental d'Apt, Haute-Provence). *Rev Micropaléontolog* 35: 91–115.

Aspotolescu V, Dellenbach J. 1999. Contribution des Ostracodes à la biostratigraphie et à la paléobiogéographie de l'Oligocène de Haute-Provence (SE France). *Géologie méditerranéenne* 26: 153–183.

Barbin V, Keller-Grünig A. 1991. Benthic foraminiferal assemblages from the Brendola section (Priabonian stage stratotype area, northern Italy): Distribution, palaeoenvironment and palaeoecology. *Mar Micropaleontol* 17: 237–254.

Blanc JJ, Masse JP, Triat JM, Truc G, Anglada R, Colom E. 1975. *Carte géologique de la France à 1/50 000, Carpentras*. Orléans: BRGM.

Bhattacharya JP. 2010. Deltas. *Facies models*, 4, 233–264.

Baudrimont AF, Dubois P, 1977. Un bassin mésogéen du domaine péri-alpin: le sud-est de la France. *Bull Centre Rech Explor Prod Elf-Aquitaine* 1: 261–308.

Bensalah M, Benest M, Truc G. 1991. Continental detrital deposits and calcretes of Eocene age in Algeria (South of Oran and Constantine). J Afr Earth Sci (and the Middle East) 12: 247–252.

Belvedere M, Fabre E, Pandolfi L, Legal S, Coster P. 2023. Stepping into Oligocene. A reassessment of the early Oligocene mammal tracks from Saignon (SE France). *Histor Biol* 1–17.

Bestani L, Espurt N, Lamarche J, Bellier O, Hollender F. 2016. Reconstruction of the Provence Chain evolution, southeastern France. *Tectonics* 35: 1506–1525.

de Bonis L. 1963. Révision de la faune de mammifères du Ludien de La Débruge (Vaucluse) (Doctoral dissertation).

Clauzade G, Roch E, Tamisier A. 1962. Les sables et argiles bigarrés du Coulon et ceux du Garry dans la région d'Apt (Vaucluse) [with discussion]. *Bull Soc Géolog France* 7: 492–497.

Clauzon G, Fleury TJ, Bellier O, Molliex S, Mocochain L, Aguilar JP. 2011. Morphostructural evolution of the Luberon since the Miocene (SE France). *Bull Soc géolog France* 182: 95–110.

Cojan I, Moreau MG. 2006. Correlation of terrestrial climatic fluctuations with global signals during the Upper Cretaceous-Danian in a compressive setting (Provence, France). *J Sediment Res* 76: 589–604.

Conard-Noireau M. 1983. La dynamique des dépots cénomaniens de Haute-Provence; observations nouvelles et implications paléogéographiques. *Bull Soc Géolog France* 7: 239–246.

Coster P, Legal S. 2021. An early oligocene fossil lagerstätten from the lacustrine deposits of the Luberon UNESCO Global Geopark. *Geoconserv Res* 4: 604–612.

Costeur L, Maridet O, Lapauze O, Mennecart B, Xiaoyu L, Roch R, .. Legal S. 2019. Le gisement oligocène de Murs, une histoire centenaire culminant sur des fouilles prometteuses. *Courrier scientifique du Parc naturel régional du Luberon et de la Réserve de biosphère Luberon-Lure* 15: 58–69.

Dèzes P, Schmid SM, Ziegler PA. 2004. Evolution of the European Cenozoic Rift System: interaction of the Alpine and Pyrenean orogens with their foreland lithosphere. *Tectonophysics* 389: 1–33.

Feist M. 1977. Étude floristique et biostratigraphique des Charophytes dans les séries du Paléogène de Provence. *Géol Méditerranéenne* 4: 109–138.

Freytet P, Plaziat J. 1982. Continental carbonate sedimentation and pedogenesis. *Contributions to sedimentology, 11*. Schweiaerbart'sche Verlagsbuchhandlung; Stuttgart.

Ford M, Stahel U. 1995. The geometry of a deformed carbonate slope-basin transition: The Ventoux-Lure fault zone, SE France. *Tectonics* 14: 1393–1410.

Germain C, Liouville M, de Bouchony P, Roch E, Demarcq G. 1966. *Carte géologique de la France à 1/50 000. Cavaillon shee*t. Orléans: BRGM.

Gierlowski-Kordesch EH. 1998. Carbonate deposition in an ephemeral siliciclastic alluvial system: Jurassic Shuttle Meadow Formation, Newark Supergroup, Hartford basin, USA. *Palaeogeogr Palaeoclimatol Palaeoecol* 140: 161–184.

Gigot P, Gubler Y, Kandel C, Triât JM, Truc G. 1975. Alpes de Provence, régions Forcalquier, Manosque, Apt, Cavaillon. In *Excursion n° 2 IXème Congr. Int. Sédim*.

Gigot P, Gubler Y, Schlund J-M. 1977. Importance et conséquences d'un système de failles syn-sédimentaires dans le bassin continental oligocène de Manosque-Forcalquier. *CR somm Soc Géol Fr* 1: 17–20.

Gigot P, Thomel G, Colomb E, Dubar M, Durozoy G, Damiani L. 1982. *Carte géologique de la France à 1/50 000, Forcalquier*. Orléans: BRGM.

Gile LH, Peterson FF, Grossman RB. 1966. Morphological and genetic sequences of carbonate accumulation in desert soils. *Soil Sci.* 101: 347–360.

Godeau N, Deschamps P, Guihou A, Leonide P, Tendil A, Gerdes A, .. Girard JP. 2018. U-Pb dating of calcite cement and diagenetic history in microporous carbonate reservoirs: case of the Urgonian Limestone, France. *Geology* 46: 247–250.

Goguel J, Dorkel M, Grégoire JY, Belleville JM, Pachoud A, Savornin J, .. & Demarcq G. 1966. *Carte géologique de la France 1/50 000 (1 feuille en coul.) et notice explicative (11 p.)-Feuille 968: Reillane*. Orléans: Bureau de recherches géologiques et minières.

Grimm KI. 2002. Foraminiferal zonation of early Oligocene deposits (Selztal Group, Latdorfian, Rupelian) in the Mainz Basin, Germany. *J Micropalaeontol* 21: 67–74.

Guendon JL. 1981. Le paléokarst du Coulon (Vaucluse, France). Sédimentation et altération d'une série détritique siliceuse sur substratum carbonate : karstification sous couverture (accumulation de gibbsite, paléosols). Thèse de 3e cycle, Marseille, 179 p.

Guendon JL, Parron C. 1983. Bauxites et ocres crétacées du sud-est de la France: mécanismes de l'altération de roches sédimentaires: *livret guide de l'excursion des 10- 11- 12 juillet 1983 organisée lors du Colloque international CNRS Pétrologie des altérations et des sols*, Paris, juillet 1983. Laboratoires des sciences de la terre.

Guyanot-Benaize C, Lamarche J, Hollender F, Viseur S, Münch P, Borgomano J. 2015. Three-dimensional structural modeling of an active fault zone based on complex outcrop and subsurface data: The Middle Durance Fault Zone inherited from polyphase Meso-Cenozoic tectonics (southeastern France). *Tectonics* 34: 265–289.

Helmer D, Vianey-Liaud M. 1970. Nouveaux gisements de rongeurs dans l'Oligocène moyen de Provence. Compte rendu sommaire des séances de la Société géologique de France, 2, 45–46

Hugueney M. 1994. *Theridomys truci* de l'Oligocène de Saint-Martin-de-Castillon (Vaucluse, France), nouvelle espèce du genre *Theridomys* (Rodentia, Mammalia) et sa relation avec la lignée de *Theridomys lembronicus*. *Scr Geolog* 104 : 115–127.

Joseph P, Cabrol C, Friès, G. 1987. Blocs basculés et passes sous-marines dans le champ de Banon (France, SE) à l'Apto-Albien: une paléotopographie directement contrôlée par la tectonique synsédimentaire décrochante. *Comptes rendus de l'Académie des sciences*. Série 2, Mécanique, Physique, Chimie, Sciences de l'univers, Sciences de la Terre, 304: 447–452.

Larsen D, Olson K. 2019. Evolution of the Pleistocene Lake Tecopa beds, southeastern California: A stratigraphic and sedimentologic perspective, in Starratt SW, and Rosen MR, eds., From Saline to Freshwater: The Diversity of Western Lakes in Space and Time: *Geological Society of America Special Paper* 536, p. 319–357.

Leeder MR. 2016. *Sedimentology and sedimentary basins: from turbulence to tectonics*. John Wiley & Sons.

Léonide P, Borgomano J, Masse JP, Doublet S. 2012. Relation between stratigraphic architecture and multi-scale heterogeneities in carbonate platforms: The Barremian-lower Aptian of the Monts de Vaucluse, SE France. *Sediment Geol* 265: 87–109.

Lesueur JL, Rubino JL, Giraudmaillet M. 1990. Organisation et structures internes des dépôts tidaux du Miocène rhodanien. *Bull Soc Géolog France* 6: 49–65.

Lesueur JL. 1991. Etude sédimentologique et stratigraphique du bassin paléogène d'Apt, Manosque, Forcalquier, Alpes de Haute-Provence, modalités de la transgression burdigalienne (Doctoral dissertation, Bordeaux 3).

Lettéron A, Fournier F, Hamon Y, Villier L, Margerel JP, Bouche A, .. & Joseph P. 2017. Multi-proxy paleoenvironmental reconstruction of saline lake carbonates: Paleoclimatic and paleogeographic implications (Priabonian-Rupelian, Issirac Basin, SE France). *Sediment Geol* 358: 97–120.

Letteron A, Hamon Y, Fournier F, Demory F, Séranne M, Joseph P. 2022. Stratigraphic architecture of a saline lake system: From lake depocentre (Alès Basin) to margins (Saint-Chaptes and Issirac basins), Eocene-Oligocene transition, south-east France. *Sedimentology* 69: 651–695.

Marty D, Meyer CA. 2006. Depositional conditions of carbonate-dominated palustrine sedimentation around the KT boundary (Facies Rognacien, northeastern Pyrenean foreland, southwestern France). *GSA Special Paper* 416: 169–187.

Ménouret B. 2014. Gisements paléontologiques à mammifères ou empreintes de pas de mammifères du Parc naturel régional du Luberon. *Courrier scientifique du Parc naturel régional du Luberon et de la Réserve de Biosphère Luberon-Lure* 12: 56–74.

Miall AD. 2010. Alluvial deposits. *Facies models* 4: 105–138.

Miall AD. 2013. *The geology of fluvial deposits: sedimentary facies, basin analysis, and petroleum geology*: Springer, 582 p.

Molliex S, Bellier O, Terrier M, Lamarche J, Martelet G, Espurt N. 2011. Tectonic and sedimentary inheritance on the structural framework of Provence (SE France): importance of the Salon-Cavaillon fault. *Tectonophysics* 501: 1–16.

Montenat C, Barrier P, Hibsch C. 2005. Enregistrement des événements pyrénéo-provençaux dans les chaînes subalpines méridionales (Baronnies, France). *Géolog France* 24.

Nel A, Garrouste R, Kaya M, Licht A, Legal S, Coster P. 2023. The second oldest representative of the genus Aeshna (Odonata: Aeshnidae) found in the lowermost Oligocene of Luberon (France) and revealed by UV light. *Histor Biol* 1–5.

Nury D, Villeneuve M, Arlhac P, Gärtner A, Linnemann U, Châteauneuf JJ, Hippolyte JC. 2016. New insights on the Marseille-Aubagne Oligocene basins (France). *Boletín Geológico y Minero* 127 (2/3): 483–498.

Page M, Licht A, Dupont-Nivet G, Meijer N, Barbolini N, Hoorn C, .. Guo Z. 2019. Synchronous cooling and decline in monsoonal rainfall in northeastern Tibet during the fall into the Oligocene icehouse. *Geology* 47: 203–206.

Pagel M, Bonifacie M, Schneider DA, Gautheron C, Brigaud B, Calmels D, Cros A, Saint-Bezar B, Landrein P, Sutcliffe C, Davis D, Chaduteau C. 2018. Improving paleohydrological and diagenetic reconstructions in calcite veins and breccia of a sedimentary basin by combining Δ47 temperature, δ18Owater and U-Pb age. *Chem Geol* 481: 1–17.

Plaziat JC. 1968. Stratigraphie continentale et sédimentologie; l'âge des couches à *'Bulimus' gerundensis* Vidal de la province de Barcelone (Espagne). *Bull Soc Géolog France* 7: 49–55.

Pirkenseer C, Spezzaferri S, Berger JP. 2010. Palaeoecology and biostratigraphy of the Paleogene Foraminifera from the southern Upper Rhine Graben and the influence of reworked planktonic Foraminifera. Palaeontogr Palaeontogr A 293: 1–93.

Rémy JA. 2000. *Plagiolophus huerzeleri*, une nouvelle espèce de Palaeotheriidae (Perissodactyla, Mammalia) de l'Oligocène inférieur (Rupélien, MP 23), à Murs (Vaucluse, France). *Geobios* 33: 489–503.

Renaut RW, Tiercelin JJ. 1994. Lake Bogoria, Kenya rift valley—a sedimentological overview. *Sedimentology and Geochemistry of Modern and Ancient Saline Lakes*, SEPM Special Publication No. 50.

Renaut RW, Gierlowski-Kordesch EH, 2010. Lakes. Facies models 4: 541–575.

Retallack GJ, Reinhardt J, Sigleo WR. 1988. Field recognition of paleosols. *Geolog Soc America Spec Paper* 216: 1–20.

Riveline J. 1986. Charophyta at the Eocene-Oligocene boundary in western Europe. *In Developments in Palaeontology and Stratigraphy.* Elsevier, Vol. 9, pp. 295-298.

Roch E. 1971. Géologie du pays d'Apt. *Bull Bur Rec geol. min*. Paris 2nd ser., 3-4, pp. 29-57.

Roberts NMW, Rasbury ET, Parrish RR, Smith CJ, Horstwood MSA, Condon DJ. 2017. A calcite reference material for LA-ICP-MS U-Pb geochronology. *Geochem Geophys Geosyst* 18: 2807–2814.

Semmani N, Fournier F, Léonide P, Feist M, Boularand S, Borgomano J. 2022. Transgressive-regressive cycles in saline lake margin oolites: paleogeographic implications (Priabonian, Vistrenque basin, SE France). *BSGF-Earth Sci Bull* 193: 8.

Semmani N, Fournier F, Suc JP, Fauquette S, Godeau N, Guihou A, Borgomano J. 2023. The Paleogene continental basins from SE France: new geographic and climatic insights from an integrated approach. Palaeogeogr Palaeoclimatol Palaeoecol 615: 111452.

Sissingh W. 2001. Tectonostratigraphy of the West Alpine Foreland: correlation of Tertiary sedimentary sequences, changes in eustatic sea-level and stress regimes. Tectonophysics 333 (3-4): 361–400.

Toumoulin A, Tardif D, Donnadieu Y, Licht A, Ladant JB, Kunzmann L, Dupont-Nivet G. 2022. Evolution of continental temperature seasonality from the Eocene greenhouse to the Oligocene icehouse-a model-data comparison. *Climate Past* 18: 341–362.

Triat JM, Truc G. 1974. Evaporites paléogènes du domaine rhodanien. *Rev Géogr Phys Géologie Dynamique* 16: 235–262.

Triat JM. 1982.*Paléoaltérations dans le Crétacé supérieur de Provence rhodanienne*. Strasbourg : Institut de Géologie – Université Louis-Pasteur. pp. 3–202. (Sciences Géologiques. Mémoire, 68).

Triat JM. 1983. Ochrification of the mid-Cretaceous glauconitic greensands in Provence, France: mineralogical sequences and facies succession. *Sci Géolog Bull Mémoires* 72: 161–167.

Truc G, Demarcq G. 1967. Eocène supérieur et Oligocène de Péréal (La Débruge-Sainte-Radegonde, près Apt, Vaucluse). Bull Soc géologique de France 7: 504–510.

Truc G. 1978. Lacustrine sedimentation in an evaporitic environment: the Ludian (Palaeogene) of the Mormoiron basin, southeastern France. *Modern and ancient lake sediments*, Spec. Publs Int. Ass. Sediment. 2, 189–203.

Vermeesch P. 2018. IsoplotR: A free and open toolbox for geochronology. Geosci Front 9: 1479–1493.

Cite this article as: Licht A, Coster P, Botté P, Kaya M, Deschamps P, Guihou A, Legal S. 2024. Sedimentology and chronostratigraphy of the Apt Basin, Southeastern France: lacustrine response to late Paleogene cooling and regional rifting, *BSGF - Earth Sciences Bulletin* 195: 22.